MONITORING AND SOURCE APPORTIONMENT OF PARTICULATE MATTER NEAR A LARGE PHOSPHORUS PRODUCTION FACILITY

Robert D. Willis and William D. Ellenson, ManTech Environmental Technology, Inc., P.O. Box 12313, Research Triangle Park, North Carolina; Teri L.Conner, National Exposure Research Laboratory, United States Environmental Protection Agency, Research Triangle Park, North Carolina

ABSTRACT

A source apportionment study was conducted to identify sources within a large elemental phosphorus plant that contribute to exceedances of the National Ambient Air Quality Standard for 24-h PM_{10}. Ambient data were collected at three monitoring sites from October 1996 through July 1999 and included the following: 24-h PM_{10} mass, 24-h $PM_{2.5}$ and $PM_{10-2.5}$ mass and chemistry, continuous PM_{10} and $PM_{2.5}$ mass, continuous meteorological data, and wind-direction-resolved $PM_{2.5}$ and PM_{10} mass and chemistry. Ambient-based receptor modeling and wind-directional analysis were employed to help identify major sources or source locations and source contributions. Fine-fraction phosphate was the dominant species observed during PM_{10} exceedances, though in general, resuspended coarse dusts from raw and processed materials at the plant were also needed to create an exceedance. Major sources that were identified included the calciners, the CO flares, process-related dust, and electric-arc furnace operations.

IMPLICATIONS

A recent federal ruling requires that the world's largest elemental phosphorus plant reduce PM_{10} emissions in several of its processes. Source apportionment results from this study suggest that the greatest reductions can be realized by eliminating the flaring or combustion of excess carbon monoxide byproduct which results in the release of P_2O_5 to the atmosphere.

INTRODUCTION

Journal of Air & Waste Manage. Assoc., in press 2001

The FMC Corporation (FMC) elemental phosphorus plant - the world's largest elemental phosphorus plant - is situated on the Fort Hall Indian Reservation near Pocatello, ID. Since October 1996, the Shoshone-Bannock Tribes, under a grant from the United States Environmental Protection Agency (USEPA) Region 10, have monitored ambient air quality on the Fort Hall Indian Reservation. Concentrations of 24-h averaged PM_{10} (particles ≤ 10 μm aerodynamic diameter), measured daily from October 1996 through March 1998, exceeded the National Ambient Air Quality Standard (NAAQS) for PM_{10} on 60 days at one or both monitoring sites immediately downwind of the FMC facility. Portions of the Fort Hall reservation have been declared a PM_{10} nonattainment area because of these violations. In addition, the area is in jeopardy of exceeding the proposed health-based NAAQS for annual and 24-h $PM_{2.5}$ (particles ≤ 2.5 μm aerodynamic diameter).[1,2] A 1995 health study[3] of persons living on the Fort Hall Reservation concluded that "the prevalence of pneumonia and chronic bronchitis was statistically significantly elevated among participants living on the Fort Hall Indian Reservation, as compared to participants living on another reservation in a remote part of Nevada".[4]

Meteorological data coupled with PM_{10} monitoring data argue strongly that FMC is the primary, if not the sole, contributor to PM_{10} levels that exceed the NAAQS in the nonattainment area.[5,6] In 1998, FMC reached an agreement with the USEPA and the Department of Justice to spend $170 million during the next four years to address environmental concerns.[6,7,8] Included in the settlement were $63 million for air quality improvements and $1.7 million for health studies with the Shoshone-Bannock Tribes.

The objective of this study was to identify major PM_{10} sources within the FMC complex so that effective control strategies could be developed and implemented. The challenge that we faced was how to perform a source apportionment study armed with high-quality ambient data from the monitoring sites, but generally lacking good source signature information. Although some signatures existed from earlier inventories (see later), subsequent operational changes at FMC raised concerns about their current validity. Several approaches were available within our time and cost constraints: 1) utilize one or more recently-developed ambient-based multivariate source apportionment models that do not require source signatures; 2) perform qualitative on-site source sampling; 3) develop off-site wind-directional sampling strategies; or 4) use some

combination of these approaches. In the end, a combination of approaches was needed to identify major emission sources and to help interpret results from source apportionment modeling. The study relied heavily on ambient particle data collected at three monitoring sites from October 1996 through July 1999. These data included (for some or all of the 34-month monitoring period): 24-h PM_{10} mass, mass and chemistry for 24-h $PM_{2.5}$ and 24-h $PM_{10-2.5}$ (particles >2.5 μm and $\leq$10 μm), continuous PM_{10} and $PM_{2.5}$ mass, continuous meteorological data (wind speed and wind direction), and $PM_{2.5}$ and PM_{10} mass and chemistry for selected wind sectors.

Phosphorus production process. A brief description of the phosphorus production process will aid the reader in understanding our receptor modeling study and its conclusions. FMC extracts elemental phosphorus from phosphorus ore, which is shipped by rail to the plant and stored on-site in large storage piles (loaves). The ore is a complex mixture containing high concentrations of P in addition to Si, Ca, Al, F, and Fe. Minor amounts of Na, K, V, Cr, and Zn, as well as trace concentrations of heavy metals (Ni, Cu, As, Se, Ba, Cd, Tl, Hg) are also likely to be present in the ore. The raw ore is screened, crushed, and pressed into briquettes which are "heat-hardened" in one of two traveling grate calciners at temperatures up to 2300 °F in order to drive off moisture and organics. Calcined briquettes, referred to as nodules, are screened to remove fines (nodule fines) which are stored in a tower. Oversized or broken nodules are pulverized by the "splitter" at one end of the proportioning building. Accepted nodules are stored in a tower for later use or are transported by conveyors directly to the proportioning building where they are blended with coke and silica to form the furnace burden. In the "burden level" of the furnace building, burden is transferred by conveyor to furnace feed bins, which feed four electric arc furnaces through gravity feed chutes. The furnaces reduce the phosphate rock matrix into elemental phosphorus (P_4), slag, and ferrophos. Slag (calcium silicate) drains to the bottom of the furnaces and is removed through slag tap holes. Hot slag exits the furnace building and cools in the slag pit located on the south side of the furnace building. From there it is transported by dump truck to a storage pile located on the south side of the FMC plant. Ferrophos (FeP) and metals such as V, Cr, and Ni which are denser than slag, are separated from the slag stream inside the furnace building and stockpiled in the ferrophos storage pile on the west side of the FMC plant. Phosphorus and CO are withdrawn from the furnaces by a vacuum pump and passed

through two condensation stages. Nearly all phosphorus is removed by condensation, while the noncondensible gases (primarily CO) are used to fire the calciners. Excess CO, beyond what is needed for calcining, is flared. A small fraction of the phosphorus is released to the atmosphere during CO flaring. Under normal conditions, CO is flared at the ground flare, but can be flared at the elevated flare when calciner demand is lower or when the secondary condenser must be bypassed. Approximately once per day, it is necessary to bypass the secondary condenser and "flush" the secondary condenser line in order to maintain efficiency in the furnace operation. During these "miniflushes," which typically last less than 50 min, flushed phosphorus is released from the elevated flare in higher concentration. Elemental phosphorus product is clarified, stored, and loaded into rail cars for shipping from a loading dock referred to as the phos dock. Captured emissions from the phos dock sumps and launder are ducted to the phos dock scrubber - another potential source of phosphorus emissions. The FMC operations described above run continuously, 365 days a year, except when relatively rare upsets occur in one of the processes. Diurnal fluctuations in plant emissions are not expected to be significant.

EXPERIMENTAL METHODS

Ambient Monitoring Design and Sample Collection

Ambient monitoring network. The Shoshone-Bannock Tribes, under a grant from the USEPA Region 10, contracted Air Resource Specialists, Inc.(ARS, Fort Collins, CO) to design, maintain, and manage the air monitoring network for the Tribes. Tribal personnel were hired by ARS to perform daily servicing for the monitors. The ambient monitoring program was designed in compliance with USEPA monitoring guidelines[9] for ambient particulate monitoring programs.

The ambient monitoring network comprises two downwind sites (Primary and Sho-Ban) and one upwind site (Background). Table 1 summarizes the experimental setup for ambient monitoring at the three sites. Figure 1 is an aerial photo of the FMC facility showing the locations of major emission sources and the Primary and Sho-Ban monitoring sites. The Primary site is located approximately 30 m north of a two-lane highway (State Highway 30) which separates the downwind monitoring sites from the FMC boundary. The Sho-Ban site is approximately 400 m

west of the Primary site and 15 m north of State Highway 30. The Background site, located 4 km west-southwest of the Primary site, was chosen to monitor background particulate concentrations in the area.

The entire FMC facility covers an estimated 1,189 acres. Due to its large size and close proximity to the downwind monitoring sites, the FMC complex subtends a large angle (roughly 80 degrees) at the Sho-Ban and Primary sites, creating a situation favorable for applying wind-direction analysis to locate emission sources. Adjoining the eastern boundary of FMC (immediately to the east of the aerial view in Figure 1) is the J.R. Simplot phosphate processing plant, which produces phosphorus-containing products including phosphoric acid and solid and liquid fertilizers. The FMC-Simplot complex is approximately 2.5 miles west-northwest of the city of Pocatello. Although Simplot emissions may significantly impact the city of Pocatello, they generally contribute minimally to PM_{10} exceedances at the Primary or Sho-Ban monitoring sites due to the strong prevailing wind pattern, as discussed below.

Meteorological data. Wind speed, wind direction, relative humidity and temperature were collected at the Primary site beginning in February 1997 using a 10-meter tower and instrumentation provided by the USEPA Region 10. One-min, 5-min, and hourly average data were collected using a Campbell Scientific CR10 Datalogger (Campbell Scientific, Inc., Logan, UT). Prior to this date, meteorological data were available from the J.R. Simplot meteorological monitoring site located about 350 m from the Primary site. A comparison of meteorological data collected simultaneously at both sites did not show significant differences in wind speed or wind direction measured at the two sites.

Continuous mass monitoring and conditional sampling. Two tapered-element oscillating microbalance (TEOM) samplers (Model 1400, Rupprecht & Patashnik Inc, Albany, NY), one equipped with a $PM_{2.5}$ inlet and the other with a PM_{10} inlet, began operation at the Primary site in November 1998. These samplers enable continuous real-time monitoring of $PM_{2.5}$ and PM_{10} mass. A data-averaging and reporting duration of 5 minutes was used for most continuous mass measurement programs.

Each TEOM instrument is coupled to an Automated Cartridge Collection Unit (ACCU, Rupprecht & Patashnik Inc.) which allows for conditional, filter-based sampling based on

preselected wind direction, wind speed, time of day, etc. During conditional sampling, the TEOM diverts part of the sampled air flow to the ACCU. This air is then directed toward any one of eight filter channels which are microprocessor-controlled. Two wind direction experiments were carried out in the present study using the ACCUs. In both studies, averaged wind direction and wind speed signals obtained from the Campbell datalogger were used to gate the ACCU channels such that air was diverted to a particular filter only when winds were from a preset direction and satisfied a minimum wind speed threshold. The wind-directional samples were collected on tared 47-mm Teflo filters (Whatman Inc., Clifton, NJ) for X-ray fluorescence analysis (XRF).

Determination of Particle Mass and Chemistry

Exposed HiVol and dichot filters were weighed to determine PM_{10}, $PM_{2.5}$, and $PM_{10-2.5}$ mass concentrations. Filters were weighed by a contract laboratory (ENSR Consulting and Engineering, Fort Collins, CO) in accordance with EPA guidelines.[9] Following weighing, dichot filters were analyzed by XRF using facilities at USEPA's National Exposure Research Laboratory (NERL) in Research Triangle Park, NC. XRF determines elemental concentrations for elements Al through U. Elements lighter than Al, including H, C, N, O, F, and compounds such as water vapor and organic carbon, are not detected in the NERL XRF system although they may comprise a significant fraction of both the fine and coarse mass. Scanning electron microscopy (SEM) combined with energy-dispersive X-ray analysis (EDX) was performed on selected source and ambient samples to yield information on the chemistry and morphology of individual particles.[10]

Qualitative Source Sampling

Source samples were collected at FMC and on the Fort Hall Reservation in March and November 1998 to generate elemental source profiles for use in interpreting wind-directional analyses and source apportionment calculations. Grab samples of dusts, soils, and raw and processed materials were ground in a mill to <10 μm, resuspended in a dust chamber, and collected on Teflon filters for XRF analysis. In addition, fine-fraction aerosol samples were collected at various locations at FMC using a portable personal air sampler (Alpha-1 Air Sampler,

E.I. duPont de Nemours & Co. Inc., Wilmington, DE) with a 25-mm filter cassette. All source samples were analyzed by XRF and SEM/EDX.

Table 2 shows the resulting XRF source profiles, expressed as elemental mass fractions. The aerosol samples are categorized as fine particles (approximately $PM_{2.5}$), and the milled dust/soil samples are coarse particles (approximately $PM_{10-2.5}$). Profiles identified by 5-digit ID numbers were collected on or near the FMC-Simplot complex in the late 1980s as part of the Pacific Northwest Source Profile Project (PNSPP)[11] and are included in the USEPA's Speciate library of source profiles.[12] (The 5-digit ID number is the Speciate profile number.) These profiles were considered quantitative when collected; however, changes in FMC operations and/or composition of the phosphate ore in the intervening years may invalidate their quantitative use in the present study. The remaining source profiles are qualitative since generally only a single sample was analyzed for each source type.

Source profiles 1–9 were collected with the personal air sampler. These include the ground flare plume before, during, and after a miniflush, the berm surrounding the ground flare pit, the phos dock, and the open traveling grate on one of the calciners. All these profiles are remarkable for their high elemental phosphorus abundance (17–24%). The phos dock profile appears to be a composite of phosphorus sources and other (possibly dust) sources. Figure 2 is an electron micrograph of a sample collected in the ground flare plume. The figure shows micron-sized, P-rich particles clinging to the fine Teflon fibers comprising the filter. These particles are very similar in chemistry and morphology to those collected at the ground flare pit, calciner grate, phos dock, and in ambient samples collected downwind of FMC. It is not known whether the phos dock and calciner grate are significant sources of fine P or whether the samplers at these sites simply picked up ambient P, which may be ubiquitous within the FMC complex. A personal sample was collected above the slag-tapping operations between furnaces 3 and 4 (profile 7). The furnace tapping profile is rich in P, K, Zn, Se, and Rb. Profile 25422, a furnace tapping profile collected at FMC for the PNSPP, differs significantly from profile 7 but was collected with more rigorous sampling procedures and may be a more accurate profile. Profile 8 was collected on the burden level (top floor) of the furnace building and shows high levels of Ca, Si, Zn, and Cd. Profile 9 was collected on the nodule fines pile and is dominated by Ca, P, and Si.

Surface dust samples were collected in the second floor of the furnace building above the hot slag tapping area (profile 10) and on the burden level (profile 11). These profiles are very similar, being dominated by Ca, Si, and P, although the slag tap area dust shows relatively higher levels of S, K, Cu, and Zn. Combustion spheres of varying composition (Al-Si-Ca, K-Ca, Ca-Si, Fe-P, Fe) were found in both locations.

Profiles 12–16 are all derived from raw or processed phosphorus ore and show considerable similarity among the major species. These sources will be difficult to resolve solely on the basis of chemistry. The profiles are dominated by Ca, P, and Si (in decreasing abundance) with an average Ca:Si ratio of 3.9. Profiles 17–21 represent coke, silica, slag, ferrophos, and crushed ferrophos. Slag is basically calcium silicate. The ferrophos profile appears to be a mixture of slag and FeP, which is not unexpected since slag and ferrophos are not cleanly separated from each other in the tapping process. The crushed ferrophos profile, in addition to Fe and P, shows unusually high levels of V, Cr, Ni and Cu. Local soil and road dust profiles are shown in profiles 22–24. Soil and road dust samples collected at the Primary site are enriched in Ca (Ca:Si = 1.3 and 1.1, respectively) relative to soil collected at the Background site (Ca:Si = 0.3), reflecting the impact of FMC at the downwind sites.

The calciner stack profile (profile 25) was generated from six duplicate calciner stack samples collected in July 1998 during stack tests conducted by FMC. Samples were collected without use of a dilution probe stack sampler. This profile can be compared to the PNSPP calciner profile (profile 25421). Although the latter profile was collected in the preferred method using a dilution probe stack sampler, the profile predates the installation of the John Zink scrubbers (a division of Koch Industries, Wichita, KS) and therefore may no longer be representative. Both calciner stack profiles are characterized by very high concentrations of P, S, Cr, Cd, and Se. Profile 25 also shows thallium at the level of 0.42%. This is the only profile for which thallium was detected. (However, we did not analyze for Tl in any of the PNSPP samples or in samples collected with the personal sampler.) SEM/EDX analysis of the calciner stack samples showed that the composition of individual particles is a mixture of S and P with significant amounts of K and Cd.

RESULTS

Meteorological Data

The wind direction at the monitoring sites is predominantly from the southwest. Figure 3 is a wind rose generated from 18,967 hourly measurements collected at the Simplot met site from 10/01/96 to 2/14/97 and at the Primary site from 2/14/97 through11/30/98. Calm winds, defined here to be hourly average wind speeds <1 ms^{-1}, account for 7.9% of all data. The sector subtended by FMC at the Primary site (160–240 degrees) accounts for one-third of all observations. Winds are infrequent from the sector subtended by the Simplot plant (90–110 degrees, approximately 2.7% of all observations). Relatively high wind speeds are associated with wind directions between 160–240 degrees: the median hourly wind speed in the 80-degree sector subtended by FMC was 5.0 ms^{-1} (11.2 mph). The average standard deviation of hourly wind direction for all samples having 24-h wind direction between 160 and 240 degrees is 25% (±50 degrees for an average wind direction of 200 degrees) showing that there is considerable variability in wind direction during a typical 24-h sampling period. This variability produces "fuzziness" which limits the ability to locate emission sources using 24-h pollutant roses.

PM_{10} Data

PM_{10} data collected concurrently at the three monitoring sites show strong local gradients. For the period 10/08/96 to 6/30/98, the average PM_{10} concentrations were 71 $\mu g/m^3$, 52 $\mu g/m^3$, and 17 $\mu g/m^3$, at the Primary, Sho-Ban, and Background sites, respectively. During this period, 47 PM_{10} exceedances were registered at the Primary site and 27 exceedances were registered at the Sho-Ban site, for a total of 61 exceedance days (13 exceedances were reported concurrently at both sites). No validated exceedances were observed at the Background site. Most exceedances occurred between October and March when 39% of the hourly wind directions were between 160 and 240 degrees compared to 26% for the remaining months.

Figure 4 shows PM_{10} roses at the three monitoring sites. All PM_{10} exceedances at the Primary site (solid circles) were associated with 24-h wind directions between 166 and 237 degrees. The mean 24-h wind direction and wind speed for exceedances at the Primary site were

200 degrees and 8.6 ms^{-1} (19 mph), respectively. Exceedances at the Sho-Ban site were associated with 24-h wind directions between 146 and 226 degrees. (Mean wind direction and wind speed were 179 degrees and 8.6 ms^{-1}, respectively). Projected backward from the Sho-Ban and Primary sites, these wind sectors encompass the major FMC facilities including the ore piles, calciners, CO flares, and the furnace building (see Fig. 1).

The ratio of Primary PM_{10} to Background PM_{10} increases from approximately 4 on non-exceedance days to 17 on exceedance days. A regression of Background site PM_{10} concentrations against same-day Primary site concentrations shows no correlation ($r^2 = 0.004$ for non-exceedance days and $r^2 = 0.0004$ for exceedance days), indicating that PM_{10} exceedances are very local in nature and are largely uninfluenced by regional background aerosol.

Alternatives to conventional pollutant roses may help extract directional information present in the data. One approach is to select a subset of samples based on a parameter of interest, e.g. 90th percentile 24-h PM_{10} concentration, then plot the frequencies of the hourly-averaged wind directions for those samples relative to all hourly wind data collected during the entire study. This method takes advantage of the higher resolution provided by hourly wind direction data to characterize the wind pattern associated with the selected parameter.[13] Figure 5 shows "relative frequency" plots for 34 exceedance samples at the Primary site and 14 exceedance samples at the Sho-Ban site. (Days for which exceedances were recorded at both sites were excluded). PM_{10} exceedances at the Primary site are seen to be associated with a 6-fold increase in the frequency of hourly winds from 190–200 degrees relative to the average frequency of hourly winds from that sector; Sho-Ban site exceedances are associated with a 7-fold increase in the frequency of hourly winds from 150–160 degrees. These peak wind sectors, projected back from the sampling sites, intersect in the vicinity of the calciners and the ground flare (Fig. 1). The last points plotted in Fig. 5 show that calm conditions are infrequent during PM_{10} exceedances.

Dichot Mass, Chemistry, and Wind-Directional Plots

Dichot mass and chemistry. Dichot samples show the relative contributions to PM_{10} mass from the fine ($PM_{2.5}$) and coarse ($PM_{10-2.5}$) size fractions and reveal differences in the aerosol chemistry of the two size fractions. This information is critical to identifying sources and

developing emission control strategies. Tables 3a and 3b summarize the mean 24-h concentrations and uncertainties for three subsets of fine and coarse-fraction dichot samples collected at the Primary site between 10/08/96 and 8/30/98. The "Non-FMC" subset includes all samples collected when the average 24-h wind direction was greater than 237 degrees or less than 166 degrees (i.e., excluding the wind sector containing all Primary site PM_{10} exceedances). The "FMC"subset includes all samples collected when the average 24-h wind direction was between 166 and 237 degrees. The labels "non-FMC" and "FMC" are intended only to suggest the dominant sources; certainly "non-FMC" samples will have some contributions from FMC sources and vice versa. The third subset consists of 13 samples collected at the Primary site during PM_{10} exceedances. Note that exceedance samples are associated with a shift in average 24-h wind direction to 193 degrees compared to the parent "FMC" subset. (Samples for which the average 24-h wind speed was <1 ms^{-1} were excluded from Table 3a).

Tables 3a and 3b show that the fine/coarse mass ratio for "FMC" and PM_{10} exceedance samples is about 1.4-1.5, compared to only 1.1 for "non-FMC" samples. Thus, the former samples are typically dominated by the fine fraction and are enriched in fine aerosol relative to "non-FMC" samples.

Fine fraction "FMC" samples are dominated by phosphorus. Assuming that the phosphorus is predominantly present as weak acidic phosphate (see discussion below), the average fine mass fraction attributable to phosphate (elemental P mass plus associated H, O, and N) is estimated to be 72% for the "FMC" samples. A scatterplot of P versus fine mass for the "FMC" samples shows a very strong correlation ($r^2 = 0.97$) which, together with phosphate's large mass fraction, indicates that phosphorus concentrations largely drive fine mass concentrations at the Primary site when winds are from the direction of FMC. Fine sulfur concentrations are typically a factor of 10 lower than phosphorus. Unusually high concentrations of thallium (Tl), selenium (Se), cadmium (Cd), and mercury (Hg) were measured at the Primary site. These elements are presumably present in trace amounts in the phosphate ore, although we have been unsuccessful in obtaining a quantitative analysis of the phosphate ore used at FMC. If the elemental concentrations in Table 3a are expressed as mass fractions, the fine-fraction

exceedance samples are seen to be enriched in P, Se, Cd, Tl, and possibly V and Hg, relative to the "non-FMC" samples.

Coarse fraction "FMC"samples and PM_{10} exceedance samples are dominated by calcium (Ca) and silicon (Si). The coarse fraction is enriched in Ca (Ca:Si = 1.2) compared to earth's crust (Ca:Si = 0.13)[14] and to the "non-FMC" samples (Ca:Si = 0.85). The "FMC" and PM_{10} exceedance samples also show unusually high concentrations of vanadium (V), chromium (Cr), strontium (Sr), and Cd. Phosphorus is quantitatively detected in only two coarse "FMC" samples; however, there is a large uncertainty associated with the need to correct for fine-fraction P collected on the coarse filter. (By design, coarse filters collect approximately 10% of the fine fraction which must be subtracted from the total filter mass in order to determine coarse concentrations). On a mass-fraction basis, coarse aerosol during exceedances is typically enriched in Ca, V, Cr, Ni, Zn, Se, and Cd, relative to "non-FMC" samples.

SEM/EDX analysis confirms the dominance of P-rich particles in fine fraction samples collected when winds are from the direction of FMC. Figure 6a is a micrograph of a fine-fraction dichot filter collected at the Primary site on 8/26/97. Particles are on the order of 1 μm in size, and nearly all are P-rich. The chemistry and morphology of these particles are very similar to that observed in source samples of the ground flare (Fig. 2) and the phos dock. Figure 6b shows the coarse-fraction mate to Fig. 6a. Most coarse particles have the rough, irregular surface morphology characteristic of crustal dust or soil particles. Particle chemistry is dominated by Ca and Si. Occasional fly ash spheres from combustion processes are observed such as the large Ca-Si-rich sphere in the upper center of the field. The fine-fraction component collected on this coarse filter can be seen in the background as small, sub-micron phosphate particles clinging to the filter fibers.

Chemistry of PM_{10} exceedances. The average PM_{10} composition during exceedances is estimated in Table 4, based on 17 dichot samples collected at either the Primary or Sho-Ban site during PM_{10} exceedances. In order to reconstruct total mass, hydrogen, nitrogen, and/or oxygen associated with XRF-detected elements must be estimated since XRF does not detect these elements. The composition of phosphate, in particular, is critical in reconstructing sample mass from XRF elemental data. Ion chromatography and pH measurements, performed on a subset of

ambient fine and coarse dichot samples, were used to establish the dominant form of ambient phosphate. Fine fraction samples were found to be mildly acidic with pH ranging from 3.2 to 5.4 in 20-ml extraction volumes. Ammonium concentrations indicated that about 50% of the acidic phosphate has ammonium ion associated with it. In constructing Table 4, therefore, we have assumed that fine phosphate is 50% H_3PO_4 and 50% $NH_4H_2PO_4$, and have corrected the elemental P concentration by a factor of 3.44 to account for the additional associated mass. Coarse P is assumed to be present as phosphate, the same as in the phosphate ore. In the absence of additional information, sulfur is assumed to be present as sulfate. The "crustal" category is the sum of the concentrations of Al, Si, K, Ca, Mn, Fe, Ti, and Sr, expressed in their common oxide states. The "metals" category sums the common oxides of V, Cr, Zn, Se, Br, and Cd – elements which are typically anthropogenic. The Background fraction is an estimate of regional (non-FMC) background contributions. It was constructed using average fine and coarse concentrations at the Background site for all days when the 24-h wind directions were between 150 and 250 degrees. Estimates of organic and elemental carbon were obtained by analyzing 11 pairs of collocated dichot samples which were collected at the Primary site on quartz filters. (None of these samples represented an exceedance day however). Organic carbon results were multiplied by 1.4 to account for total organics. For these 11 days, organic compounds and elemental carbon together accounted, on average, for only about 5% of the fine mass and 2% of the coarse mass. We have assumed the same percent mass fractions for the exceedance samples in Table 4, but show these values in parentheses to indicate the high uncertainty associated with the carbon estimates. The "Unknown" category is simply the difference between the gravimetric mass and the reconstructed mass.

As seen from Table 4, phosphate salts are estimated to account for nearly three-fourths of the fine mass and nearly half of PM_{10} during exceedances. (We assume that PM_{10} can be approximated by the sum of fine plus coarse mass). The crustal category is estimated to account for 50% of the coarse fraction, but only about 3% of the fine fraction and 23% of PM_{10}. The coarse crustal component is dominated by Ca and Si with an average Ca:Si ratio = 1.5, reflecting a strong impact from FMC. (By comparison, the Ca:Si ratio in the coarse Background component is 0.4). Sulfate is a minor component in all size fractions, accounting for only about 3% of PM_{10}

during exceedances. (Regional sulfate included in the Background category is estimated to contribute about 20% of the total sulfate in the fine fraction). Five percent of the fine mass and nearly 11% of the coarse mass is unaccounted for. This unknown component may include light elements and compounds not detected by XRF (ammonium, nitrate, water vapor, and any remaining oxygen). Some of the remaining unexplained mass in the fine fraction may be water trapped in phosphate particles. Phosphoric acid and phosphate salts are both hygroscopic, and SEM analyses of some P-rich particles provide evidence of trapped water of hydration boiling off during localized heating from the electron beam.

Wind-direction analysis of dichot samples. Relative frequency plots provide information on the direction of major emission sources. Figure 7 shows relative frequency plots for selected fine and coarse-fraction species measured at the Primary site. Note that higher wind speeds tend to dilute stack emissions so that concentrations monitored downwind may underestimate true source strengths. This effect is corrected to first order in fine species by using the product of wind speed and concentration.[15] With the exception of Br, the fine-fraction plots in Fig. 7 were constructed from the 20 samples with the highest wind-speed-corrected concentration (90^{th} percentile). Use of a 90^{th} percentile threshold improves the plot's signal-to-noise, at the cost, however, of excluding most of the data. Wind-speed-corrected fine mass, P, Se, and Cd largely track together, suggesting major sources at 170–180 degrees and 200–230 degrees. Multiple FMC sources lie in these directions including the ground and elevated flares (183 and 207 degrees respectively), calciners (193 degrees), nodule fines storage pile (223 degrees), furnace building (210-223 degrees), phos dock (223 degrees), and the slag pit (210-220 degrees). Fine K and fine Rb are highly correlated ($r^2 = 0.97$) and probably derive from the same source or sources. Both species have their highest abundance in the furnace tapping profiles (profiles 7 and 25422, Table 2), and their plots in Fig. 7 point in the direction of the furnace building. Thallium is emitted from the calciner stacks and possibly other sources; its relative frequency plot peaks broadly near 180 degrees.

For the species discussed above, Fig. 7 provides no indication of sources outside of the sector subtended by FMC. The fine Br plot however, using uncorrected 95^{th} percentile concentrations, suggests a weak source of fine Br at 100–120 degrees. All of the high-Br samples

represented in this plot were collected in the eight months between October 1997 and May 1998. Hourly wind data for these samples show that calm conditions were more than twice as likely to coincide with high Br concentrations, compared to the average frequency of calm periods over all hourly wind data. We speculate that the Simplot plant (90-110 degrees) or the city of Pocatello may be the source of the Br and that quiescent wind conditions provide favorable conditions for fine Br to accumulate to detectable concentrations at the Primary site.

Relative frequency plots for coarse species measured at the Primary site are shown on the right in Fig. 7. Coarse plots were constructed from samples having uncorrected 24-h concentrations exceeding the 90th percentile. (Coarse concentrations were not multiplied by wind speed since resuspended coarse dust concentrations are expected to increase with wind speed). All coarse plots show the same prominent peak at 170–180 degrees that was observed for many of the fine species, suggesting that this sector contains sources for both $PM_{2.5}$ and coarse particles. Slag-handling operations may explain the secondary peaks at 220–230 degrees observed for coarse mass, Ca, and Si; however, these peaks are very narrow and may not represent real sources. Coarse V and Cr are highly correlated ($r^2 = 0.94$) and have nearly identical plots, peaking strongly at 175 degrees. Coarse K and Rb, like their fine-fraction counterparts, are strongly correlated; but the coarse plots differ from the fine K and Rb plots which indicated major contributions from the direction of the furnace. Coarse Zn, however, does show a pronounced peak in the direction of the furnace building. (Zinc is abundant in the slag tap dust and slag loadout profiles).

Continuous Mass Monitoring and Wind Directional Studies

Continuous monitoring of $PM_{2.5}$ and PM_{10} began at the Primary site in November 1998 using two TEOM samplers equipped with a $PM_{2.5}$ cyclone inlet and a PM_{10} inlet, respectively. It was hoped that continuous monitoring might resolve questions about the relative importance of transient emission "spikes" versus steady-state processes at FMC, whether or not there were daily patterns in the continuous PM_{10} record that could be associated with specific FMC sources or operations, and whether PM_{10} exceedances correlated with winds from certain directions.

Continuous mass monitoring. Continuous mass data, determined every two seconds, were averaged and reported in 5-min intervals. Figure 8 shows TEOM and met data for a PM_{10} exceedance day at the Primary site (February 23, 1999). While the Primary site HiVol registered 269.9 $\mu g/m^3$ for 24-h PM_{10}, the TEOM PM_{10} and $PM_{2.5}$ monitors reported 24-h averages of 236 $\mu g/m^3$ and 165 $\mu g/m^3$, respectively. Approximately 70% of the PM_{10} was in the fine fraction for this exceedance event. The wind direction plot shows winds predominantly from 180-240 degrees and moderate wind speeds of 3-6 ms^{-1}. The cause of the $PM_{2.5}$ "event" at 16:30 hours and lasting approximately 40 minutes is not known. Although this is characteristic of a furnace upset resulting in an unplanned release of P_2O_5 from the pressure relief valves (PRVs), FMC logs show no PRV releases or furnace flushes (planned releases from the furnace PRVs) on this day.[16] It is noteworthy that the sudden drop in PM_{10} and $PM_{2.5}$ concentrations to very low values at approximately 8 AM coincides with a temporary period of calm (low wind speed and unstable wind direction). For this 1-2 h period of time, the Primary site was not strongly impacted by FMC emissions: winds were insufficient to resuspend coarse particulate matter, and any plumes containing fine PM may simply have risen and passed over the monitoring site. These data suggest that temporal variability observed in ambient PM_{10} and $PM_{2.5}$ may be driven more by changes in wind direction and/or wind speed than by changes in source emissions.

TEOM data records reveal occasional $PM_{2.5}$ events associated with unplanned pressure releases from one of the furnaces causing substantial quantities of P_2O_5 to be vented to the atmosphere. During these events, $PM_{2.5}$ concentrations at the downwind monitoring sites can approach 1000 $\mu g/m^3$ for a short time. Such upsets occur a number of times during a year, but typically do not last long enough to be the primary cause of a PM_{10} exceedance. TEOM data have been examined for PM_{10} or $PM_{2.5}$ "spikes" coincident with known times of planned miniflushes and/or furnace flaring. Generally, such spikes only stand out in the TEOM record when wind conditions are optimal for transport from the source to the Primary site. Except in rare circumstances, we think that it is unlikely that miniflushes or furnace flaring contribute more than 10% of the PM_{10} needed for an exceedance.

Five-min averages of TEOM mass and concurrent meteorological data were analyzed to investigate associations between wind direction and ambient mass concentrations. The compass

was divided into16 sectors of 22.5 degrees each. Average "mass loading" factors were determined for each sector by dividing the amount of mass associated with the chosen sector by the number of sampling periods recorded for that wind sector. Figure 9 shows the results for $PM_{2.5}$ and $PM_{10-2.5}$ for the sampling period of November 19, 1998 - June 6, 1999. Mass loadings for both size fractions are strongly peaked in the direction of FMC. However, $PM_{2.5}$ mass loadings peak in Sector 8 (180-202.5 degrees) while the $PM_{10-2.5}$ mass loadings peak in Sector 9 (202.5-225 degrees). These plots provide insight into the origins of PM_{10} exceedances. For example, average contributions from Sector 8 during the seven-month sampling period, were 174 $\mu g/m^3$ of $PM_{2.5}$ plus 79 $\mu g/m^3$ of $PM_{10-2.5}$ for a total of 253 $\mu g/m^3$ of PM_{10}. This is the daily average PM_{10} concentration at the Primary site that would be predicted if the winds originated from Sector 8 for an entire 24-hour period. Average contributions of 115 $\mu g/m^3$ of $PM_{2.5}$ plus 89 $\mu g/m^3$ of $PM_{10-2.5}$ for a total of 204 $\mu g/m^3$ of PM_{10} would be expected on days when the winds were exclusively from Sector 9. These plots also indicate a PM_{10} background from non-FMC sources of about 25 $\mu g/m^3$.

Wind directional studies. Two wind-sector sampling studies were conducted with the TEOM-ACCU samplers in order to study PM_{10} and $PM_{2.5}$ chemistry as a function of wind direction. A comparison of dichot and collocated ACCU samples unfortunately showed severe line losses of coarse fraction material between the PM_{10} TEOM sampler and its ACCU filter packs, which invalidated the ACCU PM_{10} results. The following discussion is thus limited to ACCU $PM_{2.5}$ results. The two studies -- January 27-February 19, 1999 and June 10-July 13, 1999 -- were similar in design and yielded similar results. The second study, however, provided better wind-direction resolution and improved signal-to-noise. In this study, the eight ACCU sampling channels were assigned to consecutive10-degree wind sectors spanning 160-240 degrees. (Results from the first study confirmed that the 100-140 degree sector - which includes the Simplot facility and Pocatello - was not a significant source of $PM_{2.5}$ at the Primary site). In addition, a minimum wind speed of 2 ms^{-1} was required to open any ACCU channel for sampling. In an effort to improve signal-to-noise, the TEOM data averaging interval, and hence the minimum ACCU channel switching time, was shortened from five minutes to one minute.

Figure 10 presents TEOM-ACCU $PM_{2.5}$ results from the second wind-sector sampling experiment. Plots are shown for selected elements that are known to be associated with the FMC facility. Note that elemental concentrations are expressed as a percent of the total $PM_{2.5}$ mass in each wind sector, rather than in terms of absolute mass concentrations. Elemental phosphorus comprises a fairly constant fraction of $PM_{2.5}$ (17-20%) between 180-230 degrees, suggesting that the entire FMC facility may serve as an area source for fine-fraction phosphate. (When absolute mass concentrations are plotted, P peaks between 190-210 degrees). On average, during the month-long sampling period, phosphate comprised 62% of the $PM_{2.5}$ aerosol coming from the direction of FMC, assuming partially neutralized acidic phosphate as per Table 4. Thallium and Cd are seen to peak between 190 and 210 degrees. These elements are abundant in the calciner stack profile, although Cd and Se also appear to be associated with furnace operations. Fine K and Zn, elements strongly associated with furnace operations, have very similar plots peaking between 220-230 degrees. Selenium is most enriched in aerosol coming from 200-230 degrees, suggesting contributions from both the calciners and furnace operations.

Receptor Modeling

Dichot data collected at the Primary site between October 1996 and August 1998 were input into the multivariate receptor model UNMIX[17-22] in an effort to identify major FMC sources and quantify source contributions. UNMIX is an ambient-based model that does not require source profiles. Using only ambient concentration data and assuming that ambient concentrations are a linear combination of an unknown number of sources of unknown composition, UNMIX estimates the number of sources, source compositions, and source contributions and uncertainties. The physical model for UNMIX requires that source compositions and contributions be strictly positive. UNMIX in addition assumes that for each source there are some ambient samples which have little or no contribution from that source.

Variability in the ambient data is key to success with UNMIX as with other multivariate source apportionment tools. In this regard, FMC presents a particular challenge. Because most FMC processes operate continuously (rather than turning on and off), variability in the downwind ambient data is driven to a very large extent by wind speed and wind direction. Thus, two or more

sources with chemically distinct profiles but located in the same direction from the Primary site, can be coupled by meteorology and extracted by UNMIX as a single factor with mixed composition.

Coarse and fine data from 204 dichot pairs were modeled separately with UNMIX. Each size fraction yielded a four-factor solution, shown in Table 5. UNMIX source compositions and uncertainties are shown as fractions of the average estimated source contribution. The average estimated source contributions are given in terms of absolute concentrations (ng/m^3) as well as percent of the average ambient fine or coarse mass. Only species used as fitting species in the model are listed, and those species with signal greater than twice the uncertainty are shown in bold. In general, fitting species represent species which were measured above detection limit in more than two-thirds of the samples. These tend to be species with large average concentrations and/or small measurement error. Note that even though non-negative source compositions and contributions are implicit in the UNMIX model, small negative values are possible due to error in the ambient data. (All the negative values in Table 5 are within 2 sigma of zero, where sigma is the associated uncertainty). Although UNMIX does not require source profiles, the calciner stack profile collected in 1998 (Table 2) was used to constrain the model for the fine fraction. (For each ambient sample, concentrations of fine S, K, Se, and Rb were divided into calciner (ca) contributions [S_{ca}, K_{ca}, etc.] and non-calciner (nca) contributions [S_{nca}, K_{nca}, etc.] using the element's ratio to thallium in the stack profile and assuming that all ambient thallium is emitted from the calciner stacks. The calciner and non-calciner species were then treated as independent fitting species in the model).

The validity of the profiles in Table 5 is determined by how well the profiles explain the observed ambient mass, and to what extent the profiles are consistent with all that is known about the sources and the airshed. The UNMIX factors account for 98 ± 17% and 101 ± 11% of the average observed fine and coarse mass, respectively. (Because of error in the ambient mass concentrations, the model does not account for exactly 100% of the observed mass). Identification of the profiles with actual sources is based on: comparison of the profile compositions with the qualitative source profiles in Table 2; wind-direction analysis; inter-species correlations in the ambient data; and SEM/EDX data. Because UNMIX relies on the ambient

data, the accuracy of the calculated profiles is limited by uncertainty in the ambient data. UNMIX estimates errors in the source compositions by a bootstrap method in which the solutions are computed on 100 random subsets of the ambient data.

Figure 11 shows relative frequency plots, analogous to Fig. 7, for the fine and coarse UNMIX factors. In order to enhance signal-to-noise, only ambient samples with the highest predicted mass contributions for a given factor (>90th percentile) are used in generating the relative frequency plots. The factor accounting for the most mass in the fine fraction is identified as "Calciner + Flares" based on the profile's high P, S_{ca}, K_{ca}, Cd, and Tl abundances, and the relative frequency plot which peaks between 180 and 190 degrees. This "source" is an example of two or more chemically distinct sources, located in approximately the same direction from the monitoring site, which are difficult to deconvolve because of covariance introduced by meteorology. The major sources represented in this factor are the calciners (including the stacks and the open grate) and the elevated and ground flares. In order to quantify the individual source contributions, additional constraints must be applied to the data as discussed below. The "Calciner + Flares" factor accounts for 43 ± 9% of the average fine mass and 54 ± 5% of the average fine P at the Primary site.

The fine-fraction "Furnace" factor accounts for 23 ± 4% of the average fine mass at the Primary site. Table 5 shows that most of the fine K and Rb and a large fraction of P and Cd are apportioned to this factor whose relative frequency plot peaks strongly in the direction of the furnace building. High levels of fine P, K, and Rb were measured above the slag tapping area of the furnace building, and high Cd concentrations were measured on the burden level. Other FMC sources located in a similar direction from the Primary site may be folded in with the "Furnace" factor. These include the phos dock, phos dock scrubber, and the elevated flares, all of which might be significant sources of fine phosphorus. Note that the sampling days with the highest predicted impacts from the "Furnace" factor (both fine and coarse) have relatively few periods of calm. This simply reflects the fact that winds from the direction of the furnace building are typically associated with moderately high wind speeds.

The "Simplot-Pocatello" factor is a statistically weak factor, even though it accounts for 22 ± 10% of the average fine mass. The profile shows poor signal-to-noise for all species except P

and S_{nca}. This source accounts for most of the fine sulfur not associated with the calciner stacks. The relative frequency plot indicates a possible source in the direction of the Simplot facility and the city of Pocatello. (The peak at 340-350 degrees is probably too narrow to represent a real source). Also noteworthy is the relatively high frequency of calm conditions associated with this factor. Similar conditions were found earlier to be associated with high concentrations of fine Br at the Primary site, and we speculate that the Simplot facility and/or Pocatello may be the source of these species during quiescent conditions or when winds are from the east.

The "Fine Dust" factor is statistically weak with poor signal-to-noise for all species and a highly uncertain mass contribution (11 ± 9%). This factor explains all of the Si and most of the Ca measured in the fine fraction, suggesting resuspended dust, and yet the profile is dominated by P. The Ca:Si ratio (0.7) is intermediate between phosphorus ore and soil from the Background site. The chemical profile does not match any of the measured source profiles in Table 2. The relative frequency plot, however, suggests FMC sources. This factor may represent a mixture of background and FMC sources including the fine-fraction tail of resuspended coarse dust from raw and processed materials at FMC.

UNMIX factors for the coarse fraction are less easily interpreted. The largest factor, accounting for 35 ± 5% of the average coarse mass, has been identified as "Coarse FMC Dust". The UNMIX profile resembles profile 41139 in Table 2 which represents a composite of six dust samples collected on paved roads within the FMC-Simplot complex. The UNMIX profile has high abundances of Si, P, Ca, Ti, V, Cr, and Fe. The relative frequency plot for this factor (Fig. 11) peaks between 160-210 degrees. Within this sector are numerous potential sources of coarse FMC dusts including the ore loaf and other raw material storage piles, the calciners, the proportioning building, the burden level of the furnace building, and road dust. Unfortunately, the similarity among source profiles for many of the coarse dust samples collected at FMC suggest that it will be difficult to distinguish the various sources of raw and processed phosphorus ore materials.

The "Non-FMC Dust" factor accounts for 28 ± 5% of the average coarse mass. Its relative frequency plot may indicate a weak source or sources toward the north or northwest of the Primary site. The profile has a relatively low P abundance. The Si concentration in this

factor's profile (19.7%) seems too high for wind-blown soil (see Table 2) but may be consistent with paved road dust (profile 41140). A possible source is a four-lane interstate highway (I-86) which runs east-west about 200 m north of the Primary site.

The coarse "Furnace" factor, like its fine counterpart, was identified on the basis of its relative frequency plot and the profile's high concentrations of K and Rb. It also has very high concentrations of Si and Ca which may be associated with slag loadout operations or with the nodules fine storage site. This factor may thus represent a mixture of sources comprising emissions from hot slag-tapping operations, the burden level, slag handling, and nodule fines. It accounts for 26 ± 6% of the average coarse mass.

The "Other" factor is a weak factor accounting for 13 ± 6% of the coarse mass. It is difficult to interpret this factor. The relative frequency plot suggests a source or sources at FMC in the general direction of the calciners. The profile is dominated by Ca, Si and P, but is distinguished by its high S concentration. Of the sources listed in Table 2, only the fine-fraction calciner stack profiles have greater S abundance. Perhaps this factor represents resuspended FMC dust that mixes in the air with sulfate emitted from the calciner stacks. Mamane et al.[23] observed similar S-enrichment of airborne minerals and spores due to adsorption of ambient sulfate aerosol.

The source apportionment results in Table 5 were used to estimate average source contributions to PM_{10} at the Primary site. The first column in Table 6 presents UNMIX apportionment results, as a percent of PM_{10}, averaged over all dichot pairs, assuming that PM_{10} can be approximated by the sum of fine and coarse mass. Over the entire set of dichot samples, non-FMC sources ("Simplot-Pocatello" + "Fine Dust" + "Non-FMC Dust") accounted on average for about 30% of the measured PM_{10}, while FMC sources (all remaining categories) accounted for the balance of PM_{10}. As discussed above, the "Fine Dust" factor may represent a mixture of FMC and non-FMC sources, so Table 6 probably underestimates the FMC contribution. There is considerable sample-to-sample variability in the apportionment results which is reflected in the large uncertainties.

The second column of Table 6 shows UNMIX results for nine exceedance days at the Primary site when valid dichot data exist for both the fine and coarse size fractions. Exceedances are characterized by large increases in contributions from the "Calciner + Flares" and "Coarse

FMC Dust" sources compared to all dichot samples. Together these two factors account for 65% of PM_{10} during exceedances. Although the "Furnace" contribution increases during exceedances in terms of absolute mass, it actually decreases as a percentage of PM_{10}, implying that this factor does not drive exceedances at the Primary site as much as the "Calciner + Flares" and "Coarse FMC Dust" factors. These observations are consistent with the observed shift in prevailing wind direction toward 190 degrees during Primary site exceedance events.

It seems clear that the "Calciner + Flares" factor represents at least two distinct sources which have been coupled by meteorology and common direction with respect to the Primary site. In order to estimate contributions from individual sources comprising this factor, additional constraints must be imposed on the data. The unusually high abundance of thallium in the calciner stack profile (Table 2) provides a means of quantifying the calciner stack contribution. Assuming that all ambient Tl comes from the calciner stacks, then the average calciner stack contribution to PM_{10} exceedances at the Primary Site (based on the nine exceedance samples in Table 6) is about $5 \pm 2\%$ of the PM_{10} mass. This is an upper limit estimate, since any additional sources of Tl would necessarily lower the calciner stack contribution. Referring to Table 6, this leaves a minimum contribution of $33 \pm 12\%$ for the calciner grate and the ground and elevated flares. In addition, FMC estimates that emissions from the elevated flare are roughly one-fourth of the ground flare emissions.[24] Calciner stack emissions are rich in S (9.1%) and P (6.2%). A calciner stack contribution of 5% would therefore account, on average, for about 36% of the ambient S and 2.2% of the ambient P measured at the Primary site during exceedances,

Similarly, the "Furnace" factor probably represents contributions from multiple sources (including furnace tapping, burden level, slag loadout, nodule fine storage pile, and the phos dock and phos dock scrubber) located within the same wind sector. High concentrations of fine Rb were measured in the furnace tapping profiles (profiles 7 and 25422, Table 2) and can be used to set an upper limit on PM_{10} contributions from furnace tapping operations. Taking the Rb abundance from profile 25422 (which is expected to be more accurate than the one-hour personal sample profile) and assuming that all ambient fine rubidium is due to furnace tapping operations, then the upper limit on the fine-fraction furnace tapping contribution to PM_{10} mass during exceedances is approximately $5 \pm 2\%$. This amount of fine-fraction furnace tapping would also

account for 34% of the PM_{10} potassium, 12% of PM_{10} cadmium, and 10% of the PM_{10} sulfur during Primary site exceedances, assuming the mass fractions in profile 25422. Of the 13% "Furnace" contribution to PM_{10} given in Table 6, we estimate that the remaining 8% is associated with coarse furnace tapping emissions, as well as PM_{10} emissions from the sources listed above which are in approximately the same direction from the Primary site.

CONCLUSIONS

The goal of our study was to identify and quantify the major sources at FMC that contribute to violations of the NAAQS for 24-h PM_{10} in the Fort Hall study area. This is a difficult task because FMC has numerous emission sources and quantitative source profiles were generally unavailable. Furthermore, meteorological coupling of multiple sources makes it difficult to estimate individual source contributions using ambient-based source apportionment models. By employing a combination of approaches, however, we were able to estimate PM_{10} contributions from several major sources or source clusters.

Our study yielded the following insights into the nature of PM_{10} exceedances and the aerosol chemistry associated with exceedance events.

- Fine-mode phosphorus-rich particles, believed to be partially-neutralized acidic phosphate, account, on average, for 72% of $PM_{2.5}$ and nearly 50% of PM_{10} in exceedances at the downwind sites. In general, both fine *and* coarse-fraction contributions are needed to make an exceedance.
- PM_{10} concentrations at the downwind monitoring sites are heavily influenced by local wind speed and wind direction. Exceedances at the Primary site are typically associated with a wind shift toward 190 degrees -- i.e., when the Primary site is approximately downwind of the calciners and the ground flare. PM_{10} associated with winds between 170-210 degrees (includes calciner stacks, calciner grates, the ground and elevated flares, and coarse, process-related dusts) increase dramatically during Primary site exceedances.
- Planned P_2O_5 releases resulting from miniflushes or furnace flaring operations are generally minor contributors to PM_{10} exceedances. Also, the J.R. Simplot plant and the

city of Pocatello do not contribute significantly to PM_{10} exceedances at the monitoring sites, although one or both of these may be a source of fine S and Br when winds are calm.

- Receptor model results, combined with constraints on calciner stack and furnace tapping contributions, predict the following source contributions to Primary site PM_{10} during exceedances: (1) calciner stacks: 5 ± 2%, (2) $PM_{2.5}$ furnace tapping: 5 ± 2%, (3) ground flare + elevated flare + calciner grates: 33 ± 12%, (4) processed-related coarse dust: 29 ± 18%, (5) furnace operations (excluding fine furnace tapping), burden level, slag handling, phos dock, nodule fines: 8 ± 7%, (6) background: 12 ± 7%, (7) unexplained: 8%.

These result suggest that major reductions in PM_{10} at the downwind monitoring sites can be realized by 1) reducing or eliminating all combustion or flaring of CO, and 2) improving emission controls on fugitive dust.

We hope that this study will provide some guidance to researchers engaged in similar source apportionment efforts. To our knowledge, our study is one of very few applications of the relatively-new UNMIX model in the literature. It is not uncommon in source apportionment studies that there is much greater confidence in the ambient data than in the source data. The absence of quantitative source signatures forces the modeler to acquire knowledge of the emission sources via other means in order to interpret the model results. In our study, for example, qualitative source samples and wind-directional analyses, especially relative frequency plots of key dichot species, proved indispensable in helping to identify source profiles generated by UNMIX. Size-segregated mass data provided by the dichot samplers were critical in implicating fine-mode aerosol as the major culprit in exceedance events. SEM/EDX analysis provided visual and chemical confirmation that combustion-related phosphate particles dominate the ambient fine fraction when winds are from FMC, and that these same particles were characteristic of several source samples. Finally, continuous mass monitoring coupled with real-time meteorological data, demonstrated the substantial influence of wind speed and wind direction on ambient PM_{10} levels, and showed that short-term emission spikes related to plant upsets or planned releases are generally not major contributors to exceedances.

ACKNOWLEDGMENTS

The authors acknowledge the contributions of many individuals who provided valuable assistance in this study: Lori Howell, Stan Baldwin, Roger Turner, and Farshid Farsi of the Shoshone-Bannock Tribe Air Monitoring Group, for their exhaustive efforts on the PM_{10}, dichotomous sampler, and TEOM sampling program, thus ensuring its success; Mark Tigges of Air Resource Specialists (ARS), for setting up and interfacing the TEOM samplers; Cheryl Dandel and Don Moussard, also of ARS, for daily transmittals of TEOM data; Jim Rice of FMC Corporation for assistance on obtaining source samples, for arranging tours of the facilities, and for helping to explain some of the short-term mass fluctuations; Robert Kellogg of ManTech for X-ray fluorescence analysis of samples; Fred Blanchard of ManTech for assistance with SEM and XRF analyses; Chris Hall and Steve Body of USEPA Region 10 for providing background information and program oversight; and finally Joellen Lewtas of USEPA for help in coordinating the various participants.

DISCLAIMER

The U.S. Environmental Protection Agency through its Office of Research and Development partially funded and managed the research described here under Contracts 68-D5-0049 and 68-D-00-206 to ManTech Environmental Technology, Inc. It has been subject to Agency review and approved for publication. Mention of trade names or commercial products does not constitute endorsement or recommendation for use.

REFERENCES

1. National Ambient Air Quality Standards for Particulate Matter—Final Rule. *Federal Register*, **1997**, *62(138)*, 38651–38760.

2. Air Resource Specialists, Inc. *Second Quarter 1999 Data Transmittal Report for the Shoshone-Bannock Tribes/Environmental Protection Agency Particulate Monitoring Program, Pocatello, Idaho*; Air Resource Specialists, Inc: Fort Collins, CO, September 30, 1999; p viii:

"The average of the 1997, 1998, and first and second quarters 1999 means at the Primary site is 41.1 $\mu g/m^3$, well above the 15 $\mu g/m^3$ standard. The average of the 98th percentile values at the Primary site is 149.6 $\mu g/m^3$, greater than the 65 $\mu g/m^3$ standard. Although the dichotomous samplers in this network are not EPA federal reference method monitors for $PM_{2.5}$, the data give an indication that the area may exceed the $PM_{2.5}$ standard."

3. Agency for Toxic Substances and Disease Registry. *Fort Hall Air Emissions Study: Fort Hall Indian Reservation;* Agency for Toxic Substances and Disease Registry: Atlanta, GA, November 1995.

4. Agency for Toxic Substances and Disease Registry. *Health Consultation: Air Contamination at the Eastern Michaud Flats, Pocatello, Bannock County, Idaho.* Public Comment Release; Agency for Toxic Substances and Disease Registry: Atlanta, GA, March 15, 2000.U.S. Environmental Protection Agency. *Fort Hall Source Apportionment Study: Final Report;* EPA 600/R-99/103;

5. U.S. Environmental Protection Agency, Office of Research and Development: Research Triangle Park, NC, 1999.

6. U.S. Environmental Protection Agency. Federal Rulemaking for the FMC Facility in the Fort Hall PM-10 Nonattainment Area—Proposed Rule; 40 CFR, Part 52, *Federal Register*, **1999**, *64(29)*, 7307–7355.

7. U.S. Environmental Protection Agency. Federal Rulemaking for the FMC Facility in the Fort Hall PM-10 Nonattainment Area—Proposed Rule; 40 CFR, Part 52, *Federal Register*, **2000,** *65(18),* 4465–4493.

8. FMC, EPA Settle on Idaho Facility, *Chemical and Engineering News,* October 26, **1998,** p 13.

9. U.S. Environmental Protection Agency. *Quality Assurance Handbook for Air Pollution Measurement Systems: Volume II;* Ambient Air Specific Methods, EPA-600/4-77-027a; U.S. Environmental Protection Agency: Research Triangle Park, NC, 1997.

10. Dzubay, T.G.; Mamane, Y. Use of Electron Microscopy Data in Receptor Models for PM-10. *Atmos. Environ.* **1989,** *23,* 467–476.

11. Core, J.E.; Rau, J.A.; Chow, J.C.; Watson, J.G.; Pritchett, L.C.; Frazier, C.A.; Kalman, D.; Houck, J.E.; Ward, D.; Cooper, J.A.; Redline, D. *Receptor Modeling Source Profile Development for the Pacific Northwest States: The Pacific Northwest Source Profile Library, Volume 3—Project Final Report.* State of Oregon Department of Environmental Quality: Portland, OR, 1989.

12. U.S. Environmental Protection Agency Technology Transfer Network, *http://www.epa.gov/ttn/chief/software.html#speciate/* (accessed August 2000).

13. U.S. Environmental Protection Agency. *Workshop on UNMIX and PMF As Applied to* $PM_{2.5}$; EPA 600/A-00/048; U.S. Environmental Protection Agency, Office of Research and Development: Research Triangle Park, NC, 2000.

14. Mason, B. *Principles of Geochemistry,* Wiley and Sons: New York, 1952.

15. Harrison, H. Polar Fluxgrams for Air Quality Management; *J. Air Waste Manage. Assoc.* **1991,** *41,* 1195–1198.

16. Rice, J., FMC Corporation, Pocatello, ID. Private communication, 2000.

17. UNMIX is available by request from Dr. Ron Henry, University of Southern California, Santa Barbara, CA.

18. Henry, R.C. History and Fundamentals of Multivariate Air Quality Receptor Models; *Chemom. Intell. Lab. Syst.* **1997,** *37,* 525–530.

19. Henry, R. C.; Lewis, C. W.; Collins, J. F. Vehicle-Related Hydrocarbon Source Compositions from Ambient Data: The GRACE/SAFER Method. *Environ. Science & Technology.* **1994**, **28**, 823-832.

20. Henry, R.C.; Park, E.S.; Spiegelman, C.H. Comparing a New Algorithm with the Classic Methods for Estimating the Number of Factors; *Chemom. Intell. Lab. Syst.* **1999,** *48,* 91–97.

21. Lewis, C. W.; Henry, R.C.; Shreffler, J. H. An Exploratory Look at Hydrocarbon Data from the Photochemical Assessment Monitoring Stations Networ*k, J. Air & Waste Management Asso*c., **1998**, **48**, 71 – 76.

22. Kim, B.-M.; Henry, R.C. Application of the SAFER Model to Los Angeles PM10 Data; *Atmos. Environ.* **2000,** *34,* 1747–1759.

23. Mamane, Y.; Dzubay, T.G; Ward, R. Sulfur Enrichment of Atmospheric Minerals and Spores; *Atmos. Environ.* **1992,** *26A,* 1113–1120.

24. Rice, J., FMC Corporation, Pocatello, ID. Private communication, 1998.

About the authors:

Dr. Robert Willis (corresponding author) is a principal scientist with ManTech Environmental Technology, Inc. (METI). Dr. William Ellenson is a research supervisor with METI. Dr. Teri Conner is a research chemist in the Atmospheric Methods and Monitoring Branch of the US Environmental Protection Agency. Dr. Willis can be reached by phone at (919) 541-2809 or by email: willis.robert@epamail.epa.gov.

Table 1. Ambient monitoring setup at three Fort Hall monitoring sites.

Site	Samplers	Species	Schedule	Data From – To
Primary	HiVol[a]	24-h PM_{10} mass	Daily	10/08/96–3/31/98
	"	"	6th day	4/01/98–6/30/98
	Collocated HiVol[a]	24-h PM_{10} mass	Daily	10/08/96–3/31/98
	"	"	6th day	4/01/98–6/30/98
	Dichotomous[b]	24-h $PM_{2.5}$ and PM_{coarse}	3rd day	10/08/96–2/07/98
		mass and elemental	2nd day	2/10/98–8/23/98
	Collocated dichot[b]	24-h $PM_{2.5}$ and PM_{coarse}	2nd day	2/12/98–8/23/98
		mass and elemental		
	10-m met tower[c]	WS, WD, T, RH	Continuous	2/14/97–present
	TEOM 2.5[d]	$PM_{2.5}$ mass	Continuous	11/11/98–7/23/99
	TEOM 10[d]	PM_{10} mass	Continuous	11/11/98–7/23/99
	ACCU 2.5[d]	$PM_{2.5}$ mass and elemental	Selected days	1/99–7/23/99
	ACCU 10[d]	PM_{10} mass and elemental	Selected days	1/99–7/23/99
Sho-Ban	HiVol[a]	24-h PM_{10} mass	Daily	10/08/96–3/31/98
	"	"	6th day	4/01/98–6/28/98
	Dichotomous[b]	24-h $PM_{2.5}$ and PM_{coarse}	2nd day	2/12/98–8/17/98
		mass and elemental		
Background	HiVol[a]	24-h PM_{10} mass	Daily	10/08/96–3/31/98
	"	"	6th day	4/01/98–6/28/98
	Dichotomous[b]	24-h $PM_{2.5}$ and PM_{coarse}	2nd day	2/14/98–8/21/98
		mass and elemental		

Notes:
a. Model 321C, Andersen Instruments Inc., Smyrna, GA.
b. Model 241, Andersen Instruments Inc., Smyrna, GA.
c. Model 05103 Wind Monitor, R.M. Young, Traverse City, MI.
d. Series 1400, Rupprecht & Patashnick Co., Albany, NY.

Table 2. Source profiles for the Fort Hall study. Concentrations are expressed as fractions of total sample mass.

	1 Pre-flush fine	2 Miniflush fine	3 Post-flush fine	4 Ground Flare fine	5 Phos-dock fine	6 Calciner Grate fine
Si	**0.00220**	**0.00380**	**0.01530**	**0.00660**	**0.01350**	**0.00620**
P	**0.18400**	**0.19700**	**0.23750**	**0.16750**	**0.19530**	**0.16820**
S	0.00000	0.00000	0.00110	**0.00100**	**0.00190**	**0.00330**
K	0.00010	0.00000	0.00025	**0.00070**	**0.00500**	0.00100
Ca	0.00100	**0.00140**	0.00140	**0.01150**	**0.02870**	**0.00670**
Ti	0.00000	0.00004	0.00060	0.00002	0.00025	0.00005
V	0.00000	0.00000	0.00015	0.00010	**0.00016**	0.00003
Cr	0.00004	0.00001	0.00020	**0.00012**	**0.00017**	0.00008
Mn	0.00000	0.00001	0.00025	**0.00003**	**0.00003**	**0.00004**
Fe	**0.00015**	**0.00010**	**0.00035**	**0.00130**	**0.00275**	**0.00080**
Ni	**0.00005**	**0.00002**	**0.00020**	**0.00003**	**0.00004**	**0.00005**
Cu	0.00000	0.00002	0.00025	**0.00001**	**0.00002**	0.00000
Zn	0.00010	0.00001	0.00007	**0.00020**	**0.00110**	**0.00020**
Se	0.00000	0.00000	0.00007	**0.00001**	**0.00020**	**0.00050**
Br	0.00000	0.00000	0.00004	0.00000	0.00001	0.00002
Rb	0.00001	0.00000	0.00000	**0.00003**	**0.00002**	0.00000
Sr	0.00002	**0.00003**	0.00021	**0.00003**	**0.00015**	0.00002
Cd	0.00170	**0.00150**	0.01010	**0.00050**	**0.00040**	0.00200
Hg	na	na	na	na	na	na
Tl	na	na	na	na	na	na
Pb	na	na	na	na	na	na

	7 Furnace Tap fine	25422 Furnace Tapping fine	8 Burden Level fine	9 Nodule Fines fine	10 Slag Tap Dust coarse	11 Burden Dust coarse
Si	**0.01470**	0.00562	**0.08160**	**0.05000**	**0.04340**	**0.04040**
P	**0.12680**	**0.15286**	**0.04040**	**0.06160**	**0.04380**	**0.03050**
S	**0.01750**	0.02618	**0.01690**	**0.00570**	**0.01070**	**0.00510**
K	**0.06480**	**0.09437**	**0.02510**	**0.00800**	**0.01330**	**0.00680**
Ca	**0.02220**	0.00057	**0.13980**	**0.12530**	**0.09640**	**0.08460**
Ti	0.00030	0.00000	0.00070	**0.00130**	**0.00080**	**0.00070**
V	**0.00020**	0.00008	0.00065	**0.00170**	**0.00090**	**0.00090**
Cr	**0.00030**	0.00028	**0.00080**	**0.00160**	**0.00090**	**0.00080**
Mn	**0.00005**	0.00001	**0.00020**	**0.00020**	**0.00017**	**0.00016**
Fe	**0.00450**	**0.00033**	**0.01250**	**0.01520**	**0.01520**	**0.01190**
Ni	0.00006	0.00002	**0.00014**	**0.00024**	**0.00018**	**0.00012**
Cu	**0.00010**	0.00004	**0.00013**	**0.00011**	**0.00019**	**0.00008**
Zn	**0.00890**	0.03750	**0.00730**	**0.00190**	**0.00340**	**0.00140**
Se	**0.00140**	**0.00013**	**0.00040**	0.00001	**0.00014**	**0.00004**
Br	**0.00001**	**0.00016**	0.00000	0.00000	0.00004	0.00000
Rb	**0.00050**	**0.00077**	**0.00006**	**0.00001**	**0.00008**	**0.00004**
Sr	**0.00002**	0.00003	**0.00040**	**0.00030**	**0.00030**	**0.00030**
Cd	**0.00080**	0.00234	**0.00370**	**0.00050**	**0.00040**	**0.00020**
Hg	na	0.00007	na	na	0.00000	0.00000
Tl	na	na	na	na	0.00000	0.00000
Pb	na	0.00036	na	na	0.00000	0.00003

Table 2. Continued

	12 Phosphorus Ore coarse	13 Nodules coarse	14 Green Briquette coarse	15 Nodule Fines coarse	16 Splitter Dust coarse	17 Coke coarse
Si	**0.03350**	**0.05720**	**0.02350**	**0.03020**	**0.03450**	**0.01910**
P	**0.05130**	**0.06140**	**0.05030**	**0.04640**	**0.05420**	**0.00420**
S	**0.00160**	**0.00380**	**0.00310**	**0.00160**	**0.00430**	**0.00690**
K	**0.00320**	**0.00500**	**0.00250**	**0.00310**	**0.00590**	**0.00080**
Ca	**0.11470**	**0.16780**	**0.12090**	**0.11880**	**0.13770**	**0.02440**
Ti	**0.00060**	**0.00090**	**0.00040**	**0.00060**	**0.00070**	**0.00025**
V	**0.00050**	**0.00110**	**0.00050**	**0.00070**	**0.00130**	**0.00010**
Cr	**0.00050**	**0.00100**	**0.00055**	**0.00060**	**0.00110**	**0.00009**
Mn	**0.00005**	**0.00004**	0.00000	**0.00003**	**0.00012**	**0.00003**
Fe	**0.00550**	**0.00910**	**0.00460**	**0.00570**	**0.01150**	**0.00400**
Ni	0.00002	**0.00015**	**0.00005**	**0.00010**	**0.00015**	0.00001
Cu	**0.00007**	**0.00010**	**0.00004**	**0.00006**	**0.00012**	**0.00003**
Zn	**0.00059**	**0.00100**	**0.00070**	**0.00080**	**0.00160**	**0.00008**
Se	0.00001	**0.00004**	**0.00003**	**0.00002**	0.00000	0.00001
Br	0.00001	0.00000	0.00001	0.00000	0.00000	0.00000
Rb	0.00002	**0.00003**	0.00002	**0.00002**	**0.00004**	0.00001
Sr	**0.00033**	**0.00050**	**0.00030**	**0.00040**	**0.00040**	**0.00008**
Cd	0.00005	**0.00009**	**0.00010**	**0.00010**	**0.00050**	**0.00005**
Hg	0.00000	0.00001	0.00000	0.00001	0.00000	0.00000
Tl	0.00002	0.00000	0.00001	0.00000	0.00000	0.00000
Pb	0.00000	**0.00010**	0.00000	0.00001	0.00003	0.00002

	18 Silica coarse	19 Slag coarse	20 Ferrophos coarse	21 Crushed Ferrophos coarse	22 Primary Soil coarse	23 Bkgd Soil coarse
Si	**0.13340**	**0.07520**	**0.13320**	**0.03140**	**0.08790**	**0.06240**
P	**0.00320**	**0.01320**	**0.00660**	**0.02580**	**0.03730**	**0.00200**
S	**0.00030**	**0.00230**	**0.00350**	**0.00050**	**0.00140**	**0.00010**
K	**0.00850**	**0.00520**	**0.00780**	**0.00340**	**0.00670**	**0.00480**
Ca	**0.01290**	**0.13690**	**0.07270**	**0.02420**	**0.11340**	**0.01560**
Ti	**0.00070**	**0.00090**	**0.00130**	**0.00130**	**0.00090**	**0.00070**
V	**0.00005**	**0.00070**	**0.00100**	**0.00450**	**0.00040**	**0.00002**
Cr	**0.00008**	**0.00070**	**0.00100**	**0.00400**	**0.00060**	**0.00003**
Mn	**0.00003**	**0.00009**	**0.00013**	**0.00030**	**0.00018**	**0.00013**
Fe	**0.00740**	**0.00770**	**0.01730**	**0.05780**	**0.00860**	**0.00520**
Ni	**0.00001**	**0.00013**	**0.00012**	**0.00060**	**0.00010**	0.00000
Cu	0.00000	**0.00006**	**0.00012**	**0.00070**	**0.00006**	0.00001
Zn	**0.00007**	**0.00024**	**0.00020**	**0.00040**	**0.00120**	**0.00005**
Se	0.00000	**0.00001**	0.00000	0.00000	0.00001	0.00000
Br	0.00000	0.00000	0.00000	0.00000	0.00000	0.00000
Rb	**0.00002**	**0.00002**	**0.00004**	0.00000	**0.00004**	**0.00002**
Sr	**0.00013**	**0.00050**	**0.00020**	**0.00003**	**0.00030**	**0.00006**
Cd	0.00000	0.00000	**0.00003**	0.00000	**0.00017**	0.00003
Hg	0.00000	0.00001	0.00000	0.00000	0.00001	0.00001
Tl	0.00000	0.00000	0.00000	0.00000	0.00000	0.00000
Pb	0.00000	**0.00006**	**0.00060**	0.00000	0.00002	0.00000

Table 2. Continued

	24 Primary Road coarse	25 Calciner Stack fine	25421 Calciner Stack fine	25420 Slag Loadout fine	25420 Slag Loadout coarse	41138 Paved Road Dust fine
Si	**0.07790**	**0.00018**	0.00841	0.04581	0.22462	**0.16505**
P	**0.01420**	**0.06160**	**0.10227**	**0.00858**	0.03291	**0.00692**
S	**0.00120**	**0.09090**	**0.08787**	**0.00295**	0.01002	**0.00525**
K	**0.00420**	**0.02920**	**0.01946**	**0.00723**	0.02205	**0.01639**
Ca	**0.08880**	**0.00040**	**0.00314**	**0.08308**	0.25577	**0.09523**
Ti	**0.00110**	**0.00000**	0.00003	0.00068	0.00140	**0.00340**
V	**0.00040**	**0.00020**	**0.00032**	**0.00022**	0.00047	**0.00034**
Cr	**0.00040**	**0.00080**	**0.00052**	**0.00022**	0.00130	**0.00041**
Mn	**0.00020**	0.00000	0.00001	0.00016	0.00033	**0.00087**
Fe	**0.01150**	**0.00025**	**0.00049**	0.00356	0.00989	**0.03385**
Ni	**0.00007**	**0.00001**	**0.00002**	**0.00004**	0.00032	**0.00011**
Cu	**0.00004**	**0.00020**	**0.00007**	**0.00004**	0.00008	**0.00018**
Zn	**0.00030**	**0.00160**	**0.00083**	**0.00352**	0.00861	**0.00318**
Se	0.00000	**0.00260**	**0.00305**	0.00001	0.00001	0.00001
Br	0.00000	**0.00013**	**0.00072**	**0.00002**	0.00003	**0.00002**
Rb	**0.00001**	**0.00020**	**0.00014**	0.00007	0.00016	**0.00011**
Sr	**0.00030**	**0.00000**	0.00000	**0.00035**	0.00080	**0.00035**
Cd	0.00000	**0.01990**	**0.00868**	0.00034	0.00082	**0.00018**
Hg	0.00002	0.00000	0.00000	0.00000	0.00000	0.00001
Tl	0.00000	**0.00420**	na	na	na	na
Pb	0.00000	**0.00030**	0.00018	0.00003	0.00003	**0.00069**

	41139 Paved Road Dust fine	41140 Paved Road Dust fine	41206 Ore & Road Dust fine	41206 Ore & Road Dust coarse	41207 Ore & Road Dust fine	41352 Ore & Road Dust fine
Si	**0.09644**	**0.20784**	**0.05091**	**0.09300**	**0.15014**	**0.20960**
P	**0.06863**	**0.01526**	**0.10013**	**0.11931**	**0.05320**	0.00311
S	**0.01478**	**0.00667**	**0.01031**	**0.01363**	0.00984	**0.00133**
K	**0.01260**	**0.01898**	**0.00638**	**0.00707**	**0.01484**	**0.02458**
Ca	**0.17238**	**0.10748**	**0.30662**	**0.29831**	**0.18833**	**0.04721**
Ti	**0.00179**	**0.00325**	**0.00113**	**0.00103**	**0.00213**	**0.00399**
V	**0.00258**	**0.00062**	**0.00272**	**0.00164**	0.00262	**0.00033**
Cr	**0.00211**	**0.00063**	**0.00181**	**0.00111**	0.00224	**0.00029**
Mn	**0.00041**	**0.00076**	**0.00020**	**0.00012**	0.00030	**0.00123**
Fe	**0.02614**	**0.03351**	**0.01441**	**0.00950**	**0.02355**	**0.04375**
Ni	**0.00031**	**0.00016**	**0.00034**	**0.00024**	**0.00036**	**0.00006**
Cu	**0.00019**	**0.00022**	**0.00015**	**0.00014**	**0.00025**	**0.00007**
Zn	**0.00440**	0.00313	**0.00284**	**0.00200**	0.00660	**0.00039**
Se	0.00006	0.00001	**0.00004**	**0.00006**	**0.00006**	0.00001
Br	**0.00003**	**0.00002**	0.00001	**0.00002**	0.00004	**0.00002**
Rb	0.00007	**0.00014**	0.00004	0.00003	0.00010	**0.00018**
Sr	**0.00066**	**0.00041**	**0.00091**	**0.00081**	0.00081	**0.00025**
Cd	**0.00036**	**0.00024**	**0.00025**	**0.00004**	0.00064	0.00005
Hg	0.00003	0.00001	0.00002	0.00000	0.00004	0.00002
Tl	na	na	na	na	na	na
Pb	**0.00011**	0.00025	0.00002	0.00005	0.00011	**0.00006**

Values greater than twice the analytical uncertainty are shown in **bold**.

na = not analyzed.

The eleven profiles identified by the 5-digit Speciate Library profile numbers were collected on-site or near the FMC complex as part of the Pacific Northwest Source Pr..le Project.

Table 3a. Fine-fraction concentrations at Primary site for selected conditions, 10/08/96–8/30/98 (Units = ng/m^3).

	"Non-FMC" wd<166 and wd>237 97 Samples			"FMC" 166<wd<237 63 Samples			PM_{10} Exceedances 166<wd<237 13 Samples		
	n	Mean	Unc	*n*	Mean	Unc	*n*	Mean	Unc
wd		313			209			193	
Mass	97	23962	2310	63	53018	5317	13	90770	9089
Al	42	48	35	40	148	61	10	322	100
Si	89	233	44	48	269	63	10	457	107
P	96	3984	611	63	11087	1753	13	18231	2918
S	97	670	78	63	1006	121	13	1366	164
K	97	446	52	63	825	99	13	798	97
Ca	97	202	23	63	368	44	13	604	72
Ti	24	<5.8	2.9	14	<5.3	2.7	5	6.5	2.8
V	17	<2.3	1.1	39	2.1	1.1	12	5.6	1.3
Cr	66	2.6	0.6	61	7.3	1.1	13	11.2	1.6
Mn	56	1.3	0.5	33	1.2	0.6	7	1.4	0.6
Fe	97	101	13	63	120	16	13	151	20
Ni	6	<1.2	0.6	14	<1.3	0.6	6	1.4	0.7
Cu	74	3.4	0.9	58	3.8	0.9	13	4.6	1.0
Zn	97	89	12	63	193	26	13	167	22
Se	94	34.7	4.6	61	117	16	13	197	26
Br	88	3.3	0.7	57	3.0	0.7	13	4.3	0.9
Rb	73	3.0	0.6	62	5.6	0.9	13	5.1	0.8
Sr	67	1.4	0.5	53	1.8	0.5	12	2.7	0.6
Cd	72	19.1	3.6	60	66.7	9.4	13	111	15
Hg	20	<2.4	1.2	24	4.2	1.5	7	6.4	1.8
Tl	55	4.2	0.9	57	18.0	2.6	13	31.8	4.4
Pb	50	3.2	1.3	43	4.6	1.7	11	6.4	2.0

Notes:
1. wd = average 24-h wind direction.
2. Samples with 24-h wind speed <1 m/s were omitted.
3. *n* = number of detections = number of samples for which concentration >2x measurement uncertainty.
4. Mean = average over all samples (detects plus non-detects).
5. Unc = measurement uncertainty averaged over all samples.
6. Values preceded by < were detected in fewer than one-third of the samples.

Table 3b. Coarse-fraction concentrations at Primary site for selected conditions, 10/08/96–8/30/98 (Units = ng/m^3).

	"Non-FMC" wd<166 and wd>237 97 Samples			"FMC" 166<wd<237 63 Samples			PM_{10} Exceedances 166<wd<237 13 Samples		
	n	Mean	Unc	*n*	Mean	Unc	*n*	Mean	Unc
wd		313			209			193	
Mass	97	21792	2296	63	36971	4283	13	58987	6900
Al	94	688	217	63	1052	332	13	1832	573
Si	97	3267	867	63	4990	1331	13	7814	2085
P	18	<983	491	2	<2650	1325	0	<4374	2187
S	96	189	43	63	364	77	13	555	113
K	97	391	60	63	653	105	13	1060	161
Ca	97	2782	332	63	5825	722	13	9060	1123
Ti	92	43.1	8.4	63	71.3	12.7	13	120.3	21.1
V	77	12.2	2.8	63	42.6	7.3	13	79.6	13.3
Cr	96	14.7	2.6	63	45.4	7.5	13	85.6	14.1
Mn	97	8.6	1.4	63	9.9	1.6	13	16.2	2.4
Fe	97	466	64	63	704	99	13	1151	162
Ni	46	1.9	0.8	61	7.1	1.4	13	13.4	2.2
Cu	71	3.0	0.9	61	5.5	1.2	13	8.6	1.6
Zn	97	34.8	6.5	63	80.4	14.9	13	124	21
Se	8	<1.8	0.9	22	5.8	2.9	6	11.2	4.9
Br	54	0.9	0.5	42	1.4	0.5	12	2.5	0.7
Rb	78	2.0	0.5	63	3.4	0.7	13	5.4	0.9
Sr	97	9.2	1.3	63	20.0	2.6	13	31.7	4.0
Cd	33	3.5	2.1	57	14.4	3.7	13	28.1	5.9
Hg	7	<1.8	0.9	11	<2.1	1.0	4	<2.5	1.2
Tl	0	<1.0	0.5	4	<1.4	0.7	2	<2.0	1.0
Pb	4	<1.9	0.9	3	<2.1	1.0	0	<2.3	1.1

Notes:
1. wd = average 24-h wind direction.
2. Samples with 24-h wind speed <1 m/s were omitted.
3. *n* = number of detections = number of samples for which concentration >2x measurement uncertainty.
4. Mean = average over all samples (detects plus non-detects).
5. Unc = measurement uncertainty averaged over all samples.
6. Values preceded by < were detected in fewer than one-third of the samples.

Table 4. Estimated $PM_{2.5}$, $PM_{(10-2.5)}$, and PM_{tot} composition for PM_{10} exceedances (in percent).

	$PM_{2.5}$	$PM_{(10-2.5)}$	PM_{tot}[1]
Phosphate[2]	72	15	49
Crustal	3	50	23
SO_4	3	3	3
Metals	1	1	1
Background	11	18	14
Organic +Elemental Carbon[3]	(5)	(2)	(4)
Unknown	5	11	6
Measured Mass ($\mu g/m^3$)	88.3	62.3	150.6

[1]PM_{tot} (= $PM_{2.5}$ + $PM_{10-2.5}$) is assumed to approximate PM_{10}.
[2]Assume 50% H_3PO_4 + 50% $H_2NH_4PO_4$ for $PM_{2.5}$, and PO_4 for PM_{10}.
[3]Carbon estimates are shown in parentheses to indicate a low degree of confidence.

Table 5. UNMIX source compositions and source contributions determined from 204 Primary site dichot pairs.

Fine Fraction Source Compositions (mass fraction ± uncertainty)				
Fine Species	**Source 1 Calciner+Flares**	**Source 2 Furnace**	**Source 3 Simplot-Pocatello**	**Source 4 Fine Dust**
Si	-0.00236 ± 0.00322	0.00085 ± 0.00251	0.00282 ± 0.00163	0.08057 ± 0.47064
P	**0.22819 ± 0.02219**	**0.22424 ± 0.01366**	**0.10610 ± 0.02338**	0.10206 ± 0.40962
S_{ca}	**0.01338 ± 0.00366**	-0.00115 ± 0.00063	-0.00043 ± 0.00024	-0.00043 ± 0.00243
S_{nca}	0.00789 ± 0.00791	**0.01737 ± 0.00347**	**0.05868 ± 0.01249**	-0.00716 ± 0.17944
K_{ca}	**0.00430 ± 0.00118**	-0.00037 ± 0.00020	-0.00014 ± 0.00008	-0.00014 ± 0.00078
K_{nca}	0.00364 ± 0.00345	**0.04785 ± 0.00768**	-0.00044 ± 0.00094	0.01570 ± 0.09979
Ca	0.00157 ± 0.00183	**0.00730 ± 0.00172**	-0.00111 ± 0.00145	0.05316 ± 0.37001
Se_{ca}	**0.00038 ± 0.00011**	-0.00003 ± 0.00002	-0.0000 1± 0.00001	-0.00001 ± 0.00007
Se_{nca}	**0.00278 ± 0.00053**	**0.00222 ± 0.00036**	0.00048 ± 0.00037	-0.00196 ± 0.01736
Rb_{ca}	**0.00003 ± 0.00001**	0.00000 ± 0.00001	0.00000 ± 0.00001	0.00000 ± 0.00001
Rb_{nca}	0.00003 ± 0.00002	**0.00034 ± 0.00006**	0.00001 ± 0.00001	0.00007 ± 0.00043
Cd	**0.00175 ± 0.00054**	**0.00104 ± 0.00037**	-0.00036 ± 0.00018	0.00064 ± 0.00621
Tl	**0.00062 ± 0.00017**	-0.00005 ± 0.00003	-0.00002 ± 0.00001	-0.00002 ± 0.00011
Average Fine Fraction Source Contributions ± Uncertainty				
ng/m³	**13828 ± 2922**	**7264 ± 1373**	**7143 ± 3179**	3412 ± 3027
% of Avg Fine Mass	**43.0 ± 9.1**	**22.6 ± 4.3**	**22.2 ± 9.9**	**10.6 ± 9.4**

Coarse Fraction Source Compositions (mass fraction ± uncertainty)				
Coarse Fraction	**Source 1 Coarse FMC Dust**	**Source 2 Non-FMC Dust**	**Source 3 Furnace**	**Source 4 Other**
Al	**0.03047 ± 0.00220**	**0.04924 ± 0.00595**	**0.02014 ± 0.00345**	**0.01395 ± 0.00442**
Si	**0.12117 ± 0.00695**	**0.19736 ± 0.01616**	**0.14453 ± 0.01243**	**0.09560 ± 0.01280**
P	**0.06703 ± 0.00721**	**0.00815 ± 0.00379**	**0.03189 ± 0.00930**	**0.02986 ± 0.00789**
S	**0.00808 ± 0.00119**	**0.00151 ± 0.00163**	**0.00832 ± 0.00237**	**0.03440 ± 0.00975**
K	**0.01652 ± 0.00150**	**0.01646 ± 0.00194**	**0.02592 ± 0.01018**	0.00628 ± 0.00381
Ca	**0.16005 ± 0.00965**	**0.06891 ± 0.01569**	**0.19967 ± 0.02073**	**0.12912 ± 0.02203**
Tl	**0.00205 ± 0.00014**	**0.00294 ± 0.00036**	**0.00155 ± 0.00027**	0.00065 ± 0.00033
V	**0.00182 ± 0.00020**	0.00000 ± 0.00013	**0.00070 ± 0.00018**	0.00019 ± 0.00012
Cr	**0.00198 ± 0.00024**	-0.00007 ± 0.00014	**0.00076 ± 0.00024**	**0.00027 ± 0.00013**
Mn	**0.00018 ± 0.00005**	**0.00079 ± 0.00011**	**0.00016 ± 0.00004**	**0.00027 ± 0.00007**
Fe	**0.02026 ± 0.00185**	**0.03282 ± 0.00510**	**0.00991 ± 0.00287**	**0.01911 ± 0.00614**
Zn	**0.00232 ± 0.00025**	-0.00004 ± 0.00035	**0.00354 ± 0.00098**	0.00028 ± 0.00036
Rb	**0.00008 ± 0.00001**	**0.00008 ± 0.00001**	**0.00015 ± 0.00006**	**0.00004 ± 0.00002**
Average Coarse Fraction Source Contributions ± Uncertainty				
ng/m³	**8717 ± 1249**	**7000 ± 1300**	**6403 ± 1480**	**3172 ± 1440**
% of Avg Coarse Mass	**34.7 ± 5.0**	**27.9 ± 5.2**	**25.5 ± 5.9**	**12.6 ± 5.7**

Notes:
1. For a given source and species, the mass fraction is the average amount of the species associated with that source, expressed as a fraction of the estimated source contribution (ng/m³).
2. (S, K, Se, Rb)$_{ca}$ and (S, K, Se, Rb)$_{nca}$ refer to species associated with calciner stack emissions (ca) and non-calciner sources (nca), respectively. See text for details.
3. Values in **bold** have signal/noise > 2.

Table 6. Estimated UNMIX source contributions to PM_{10} at the Primary site.

UNMIX Factor	Average Contribution ± Uncertainty (% of PM_{10})	
	203 Dichot Pairs	9 Exceedance Days
"Calciner + Flares"	24 ± 5	38 ± 12
"Furnace" (fine+coarse)	24 ± 4	13 ± 7
"Coarse FMC Dust"	15 ± 2	27 ± 18
"Non-FMC Dust"	12 ± 2	2 ± 5
"Simplot-Pocatello"	12 ± 6	4 ± 3
"Fine Dust"	6 ± 5	6 ± 3
"Other"	6 ± 3	2 ± 3

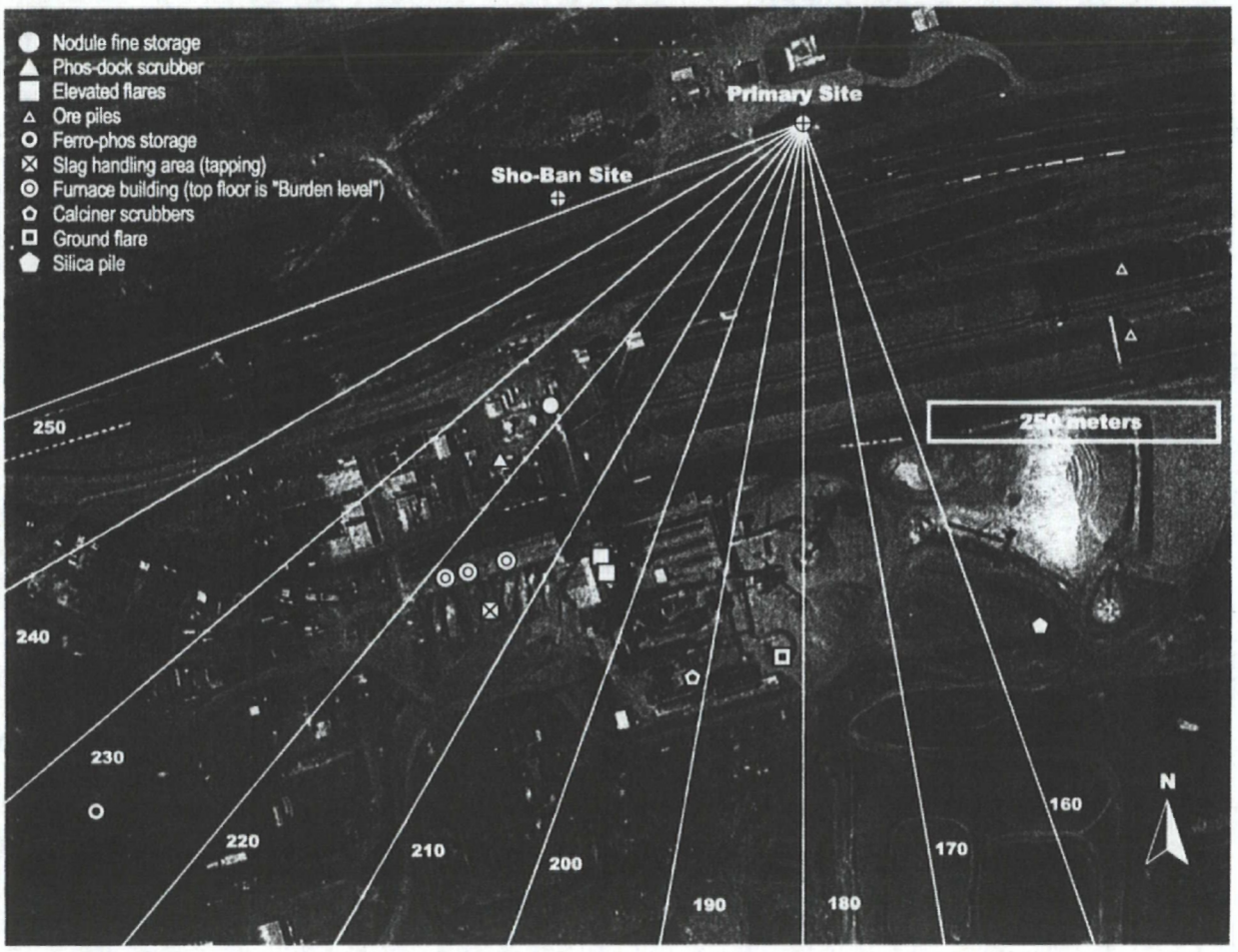

Figure 1. Aerial view of the Fort Hall study area showing the FMC complex and the Primary and Sho-Ban monitoring sites.

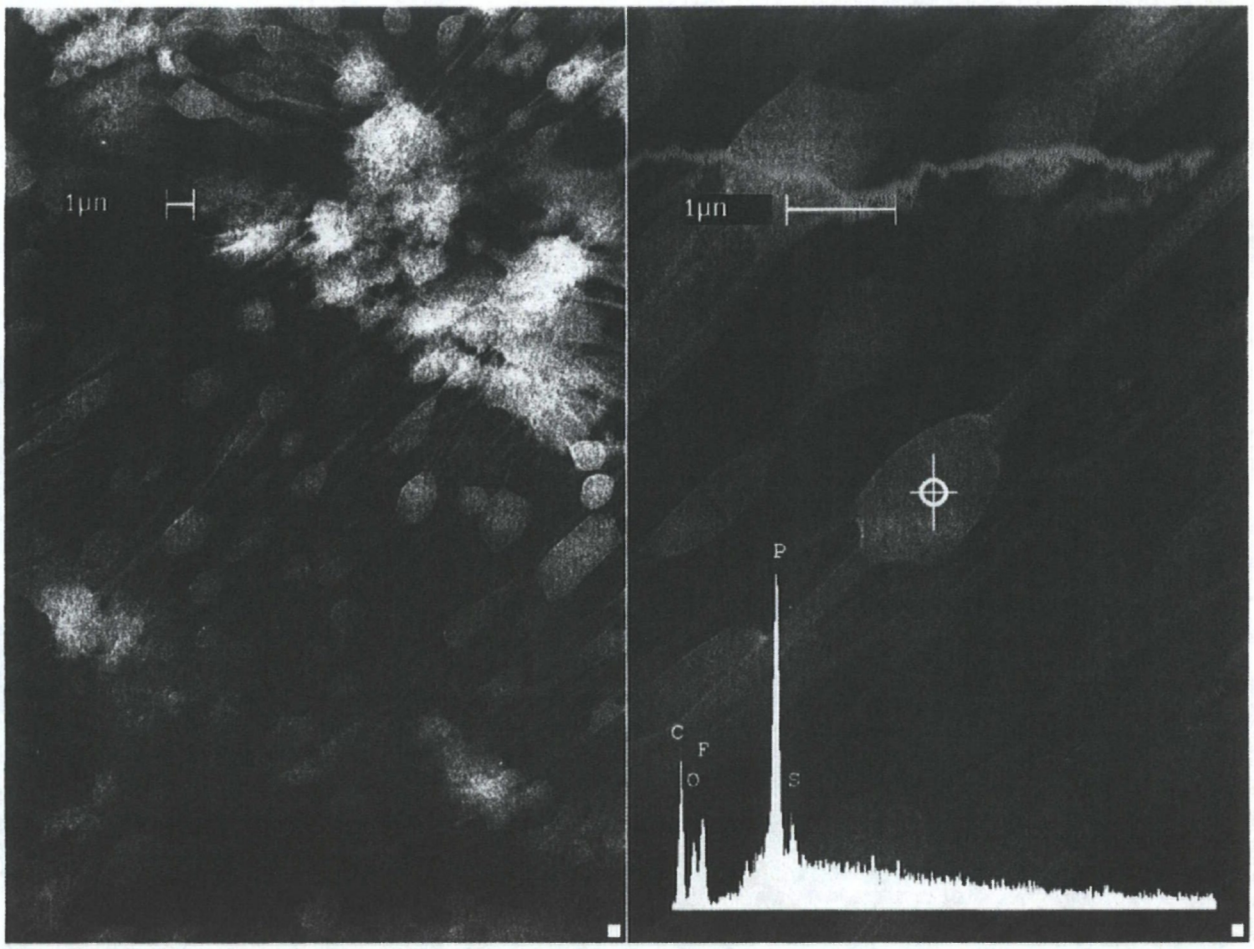

Figure 2. Personal air sample collected from the ground flare plume during a miniflush. Particles are approximately 1 micron in size and cling to fine Teflon fibers comprising the filter. Nearly all particles are droplet-like P-rich particles similar to the one centered in the magnified image on the right. Large clumps of white are Teflon ribs which provide structural support for the membrane filter.

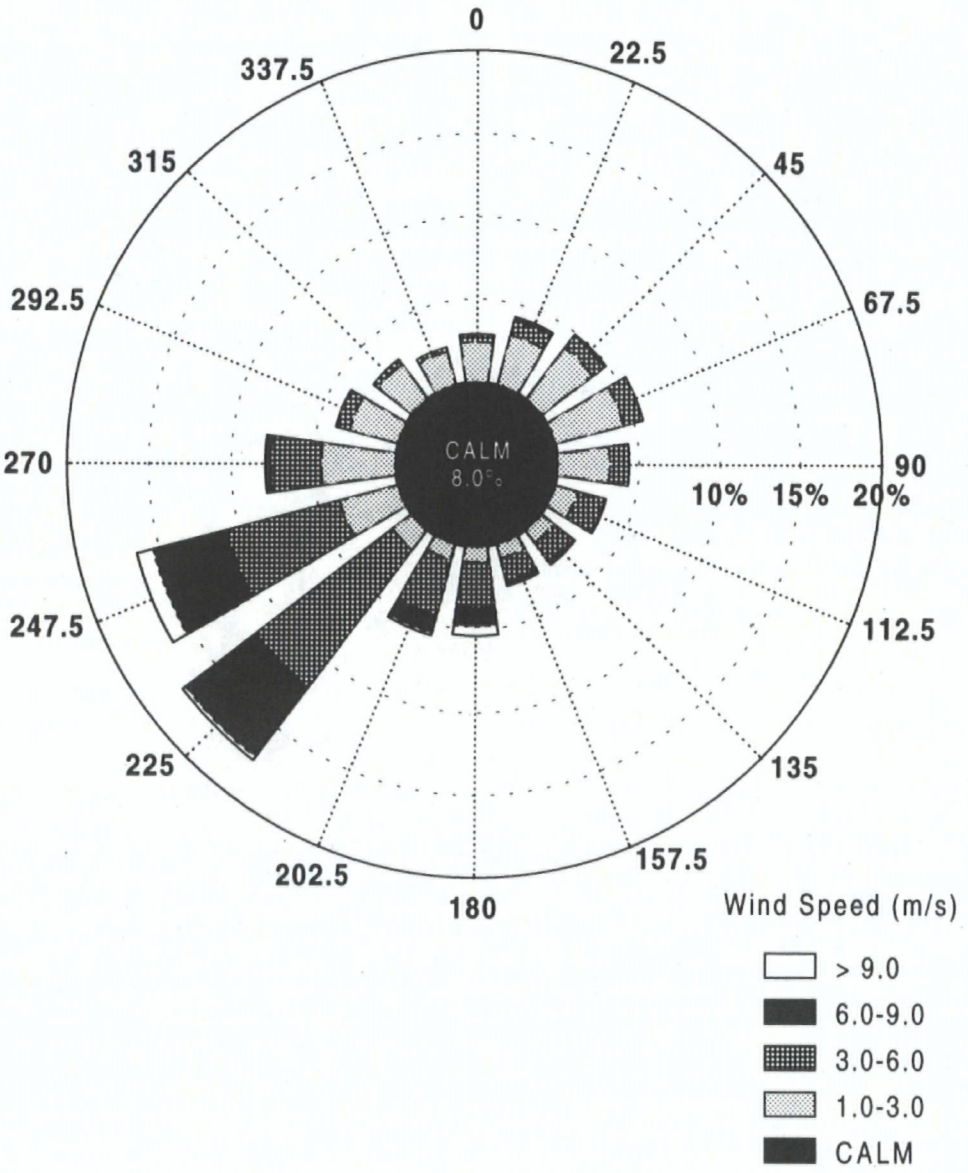

Figure 3. Primary site wind rose for hourly-averaged wind speed and wind direction. Data were collected between 10/01/96 and 11/30/98.

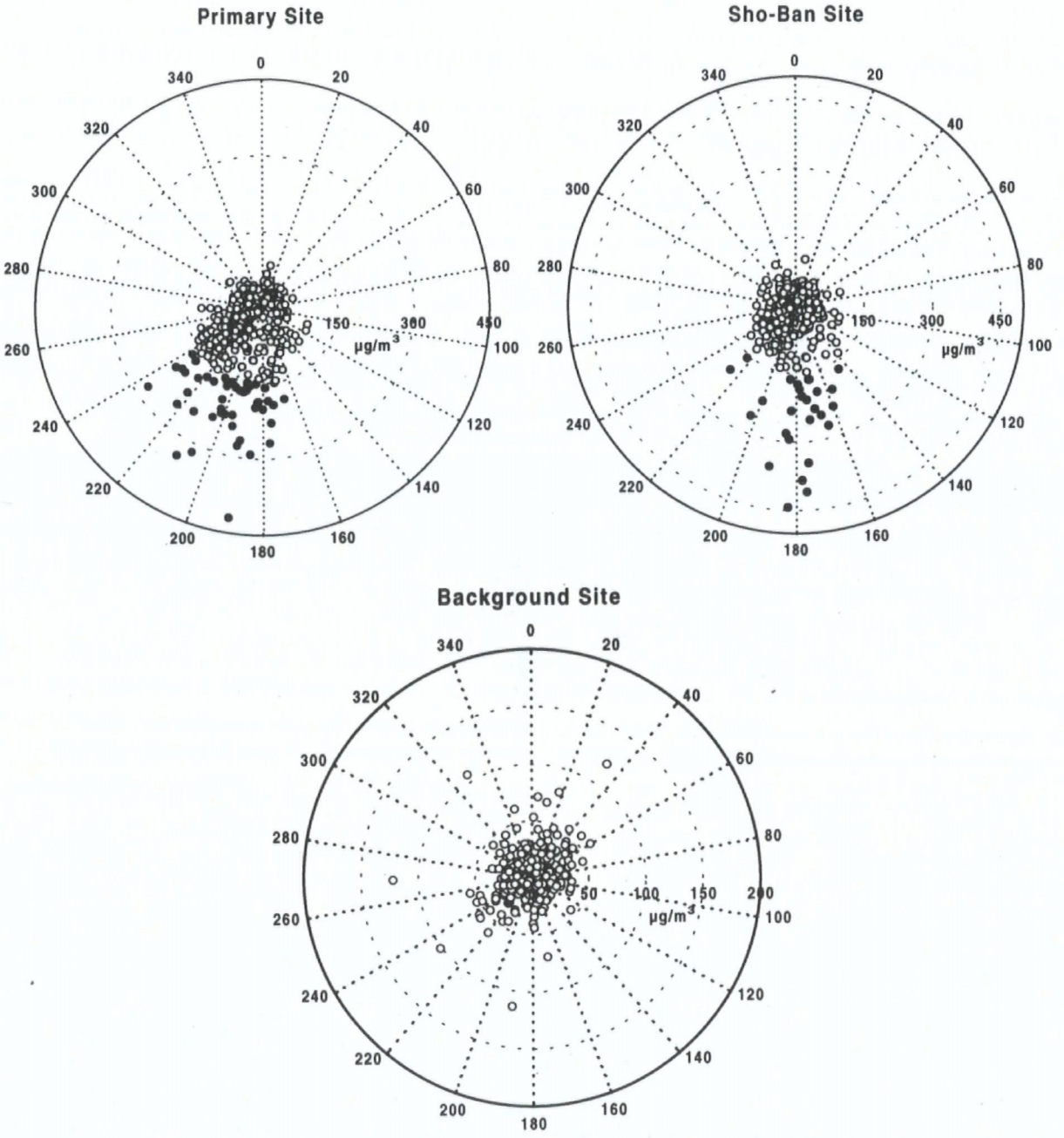

Figure 4. PM_{10} roses at the Primary, Sho-Ban, and Background monitoring sites for samples collected between 10/08/96 and 6/30/98. The radial amplitude is proportional to the 24-h PM_{10} concentration. Solid data points are PM_{10} exceedances.

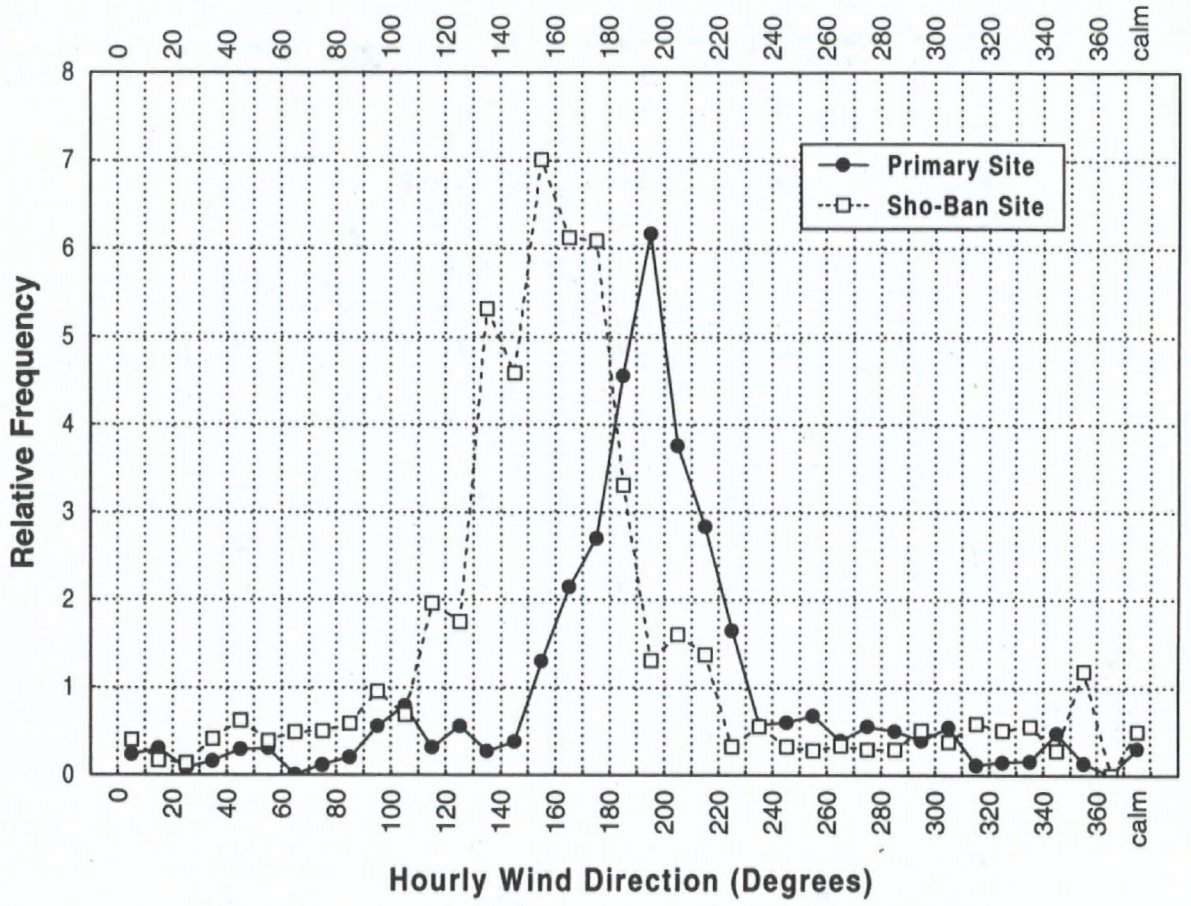

Figure 5. Relative frequency plots for 24-h PM_{10} exceedance samples at the Primary and Sho-Ban sites. Plot resolution is 10 degrees. Hourly-averaged wind direction data were compiled from 34 sampling days for which exceedances were recorded only at the Primary site (solid curve) and 14 days for which exceedances were recorded only at the Sho-Ban site (dashed curve). The vertical scale shows the frequency of hourly wind directions from a given 10° sector relative to all hourly data for that wind sector.

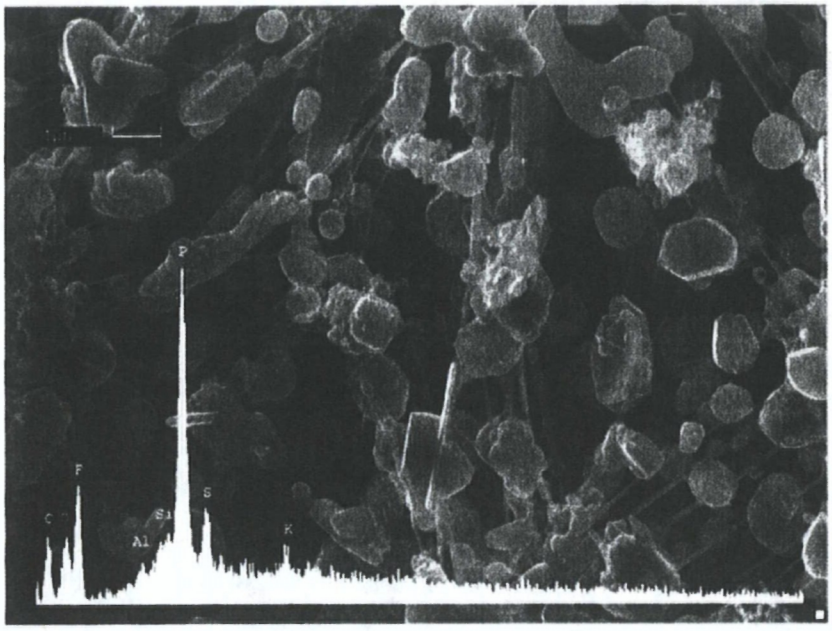

Figure 6a. Fine dichot sample collected at the Primary site (8/26/97). The superimposed x-ray spectrum, acquired by rastering the electron beam over the entire field, shows that nearly all particles are phosphorus-rich. (The fluorine and carbon peaks are generated by the Teflon filter).

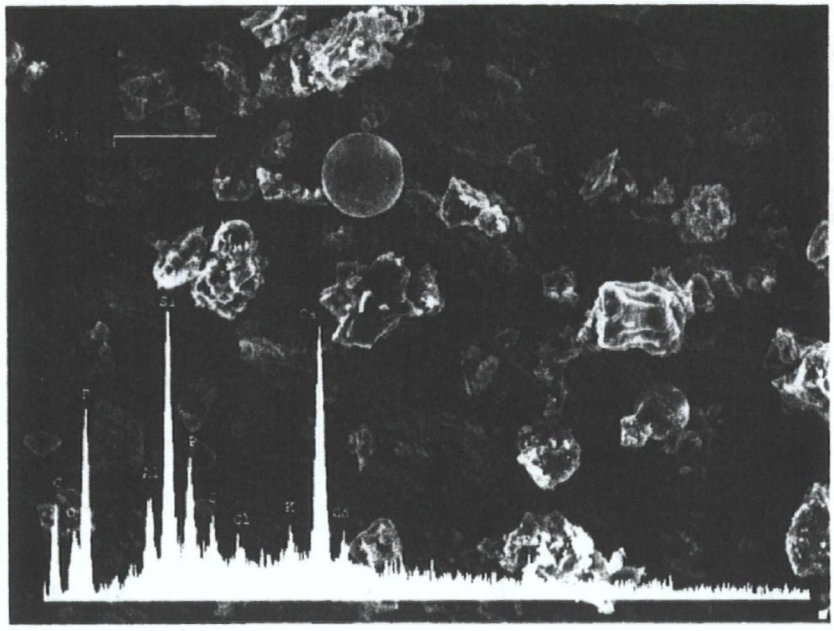

Figure 6b. Coarse dichot sample collected at the Primary site (8/26/97). Coarse particle chemistry is dominated by Ca and Si. Spherical particles such as the large Ca-Si-rich sphere in the upper center of the field are produced in combustion processes.

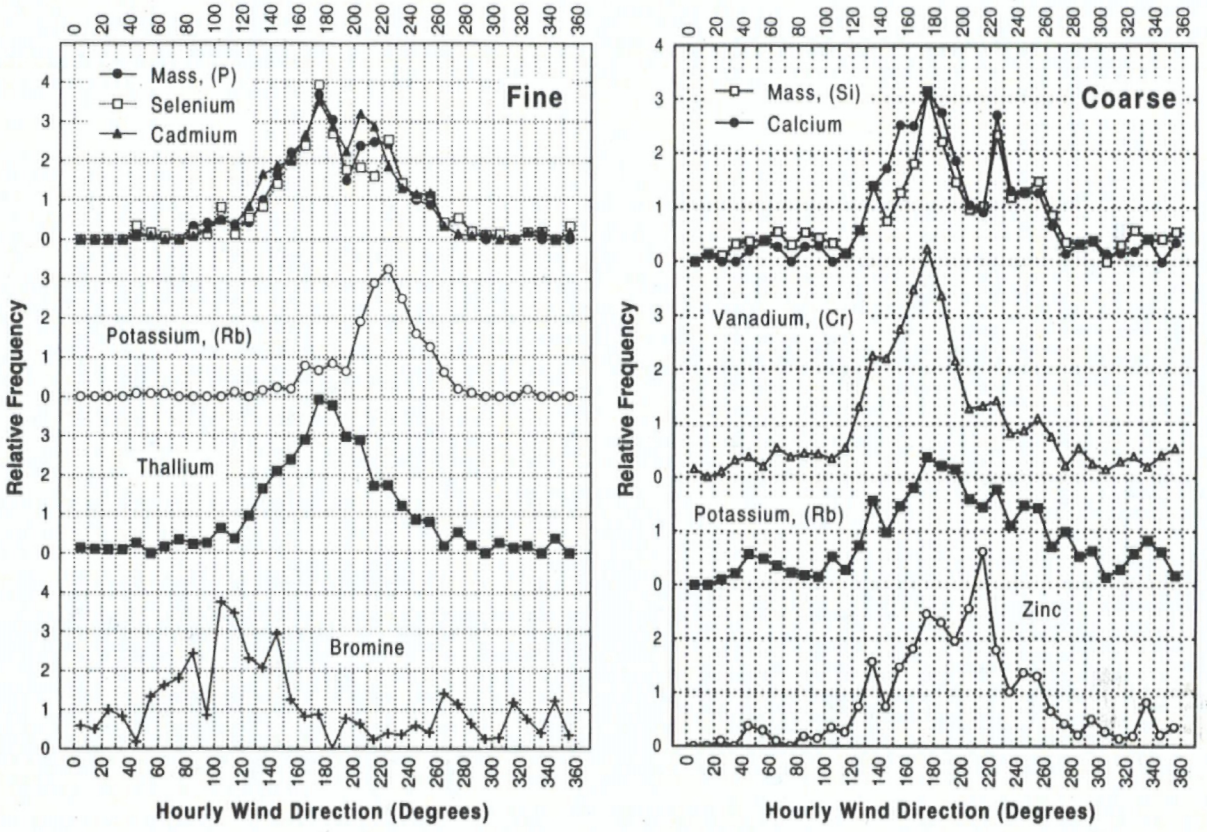

Figure 7. Relative frequency plots for selected fine and coarse dichot species at the Primary site. The fine Br plot was constructed from samples having Br concentrations exceeding the 95th percentile. Samples with 24-h wind-speed-corrected concentrations exceeding the 90th percentile were selected for all other fine species. Fine P and fine Rb plots were nearly identical to fine mass and fine K, respectively, and were not plotted. Coarse plots were constructed from samples with uncorrected 24-h concentrations exceeding the 90th percentile. Coarse Si, Cr, and Rb plots were nearly identical to plots of coarse mass, coarse V, and coarse K, respectively.

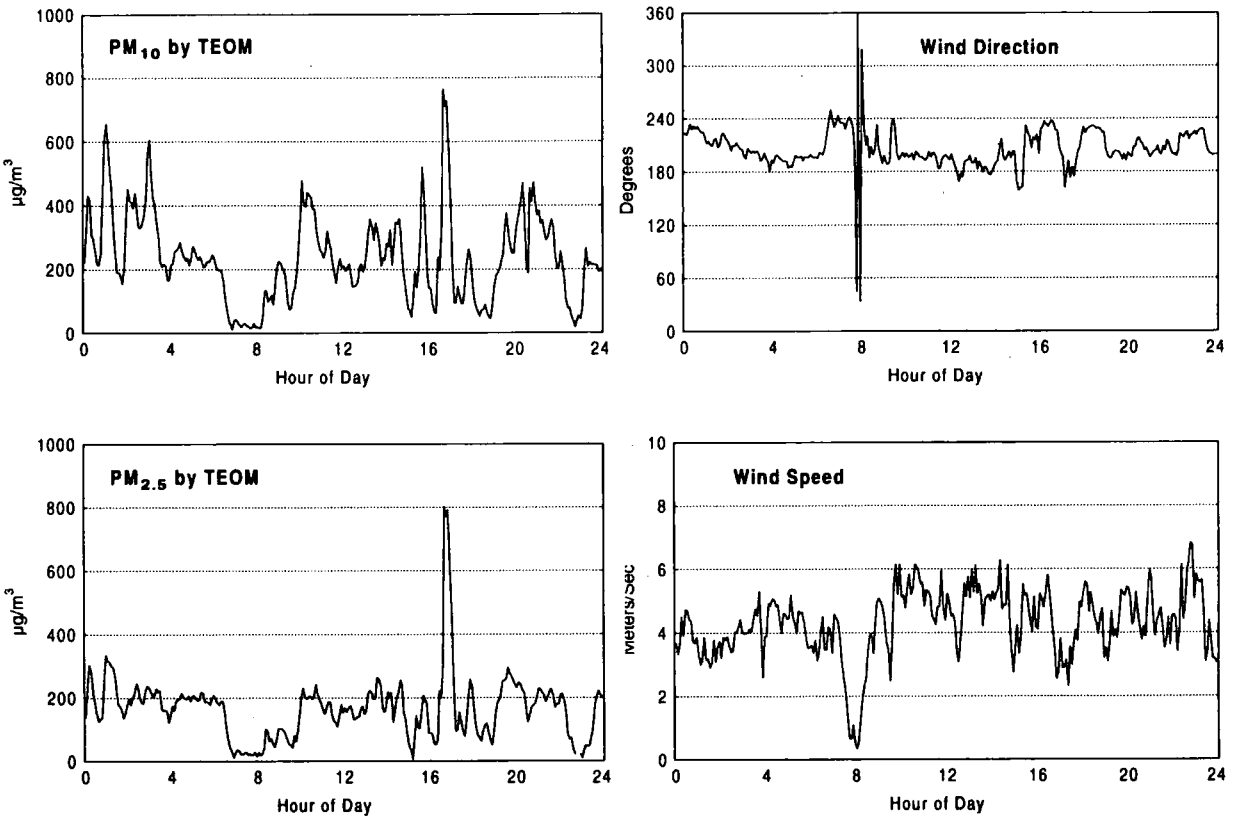

Figure 8. Five-minute average TEOM PM_{10}, TEOM $PM_{2.5}$, wind speed, and wind direction for a PM_{10} exceedance day at the Primary site (2/23/99). The HiVol monitor registered 269.9 $\mu g/m^3$ for the day. Note the precipitous drop in aerosol concentrations coinciding with calm conditions at about 8 am.

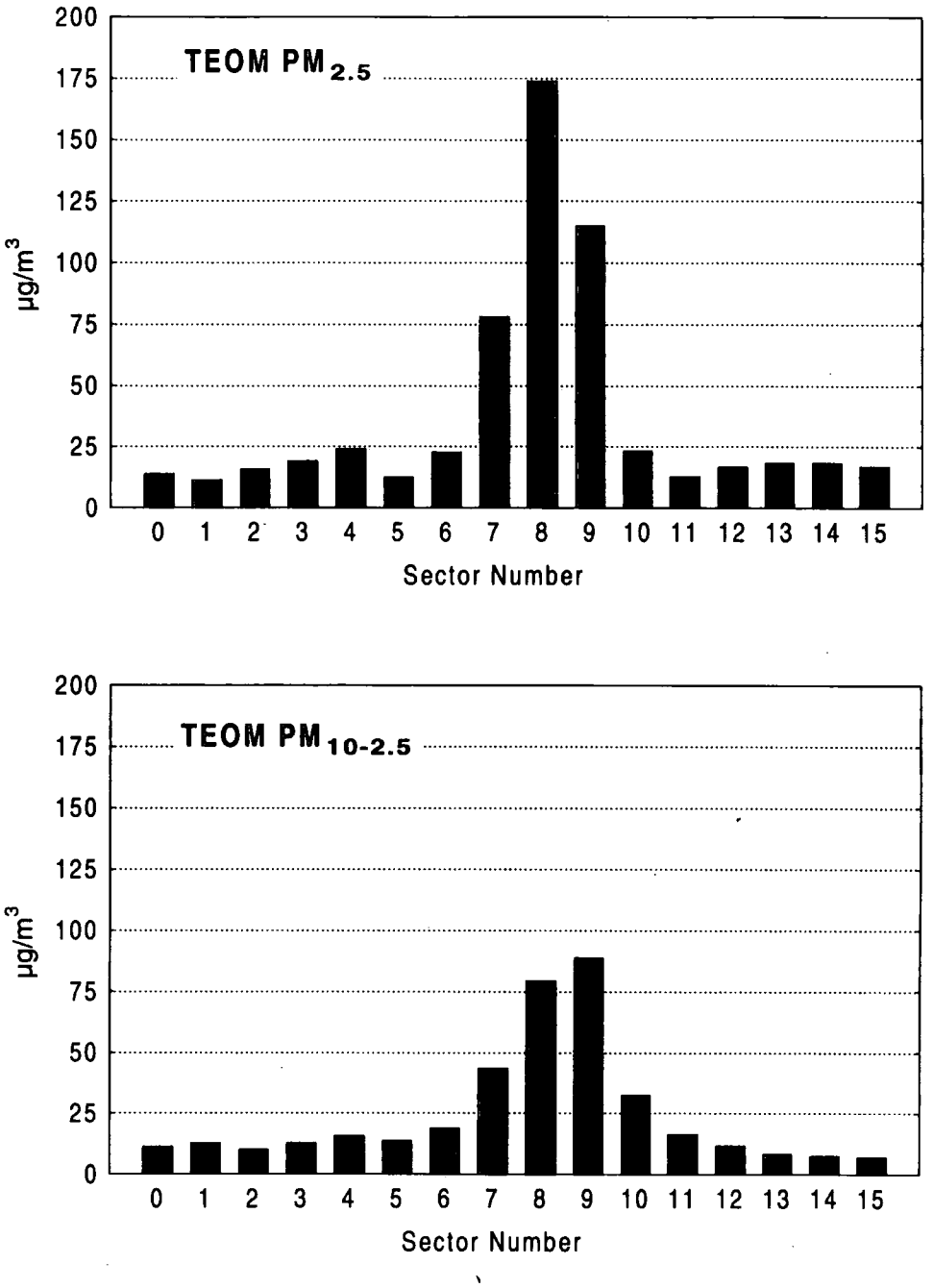

Figure 9. Continuous $PM_{2.5}$ (top) and $PM_{10-2.5}$ (bottom) mass results, averaged by wind sector, for November 19, 1998 - June 6, 1999. Coarse ($PM_{10-2.5}$) concentrations were calculated as the difference between TEOM PM_{10} and TEOM $PM_{2.5}$ concentrations. Wind sectors are contiguous 22.5-degree sectors with Sector 0 representing 0-22.5 degrees. $PM_{2.5}$ mass loadings peak sharply in Sector 8 (180-202.5 degrees) while coarse mass loadings peak in Sector 9 (202.5-225 degrees).

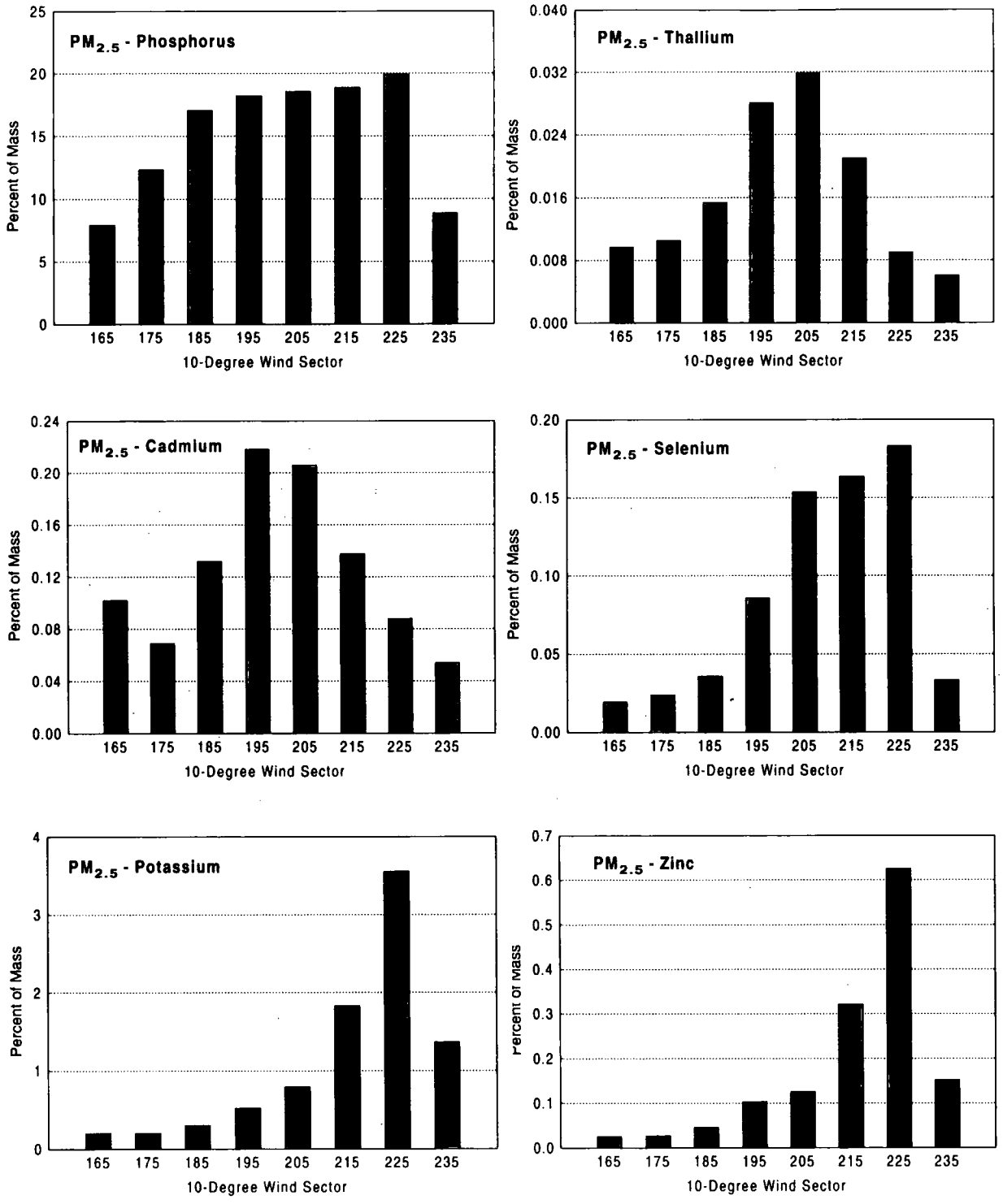

Figure 10. Percent of $PM_{2.5}$ mass versus wind sector for selected species measured at the Primary site. Each 10-degree sector was assigned to a separate ACCU channel which collected aerosol only when the 1-min average wind direction was from the assigned sector and the 1-min average wind speed exceeded 2 ms^{-1}.

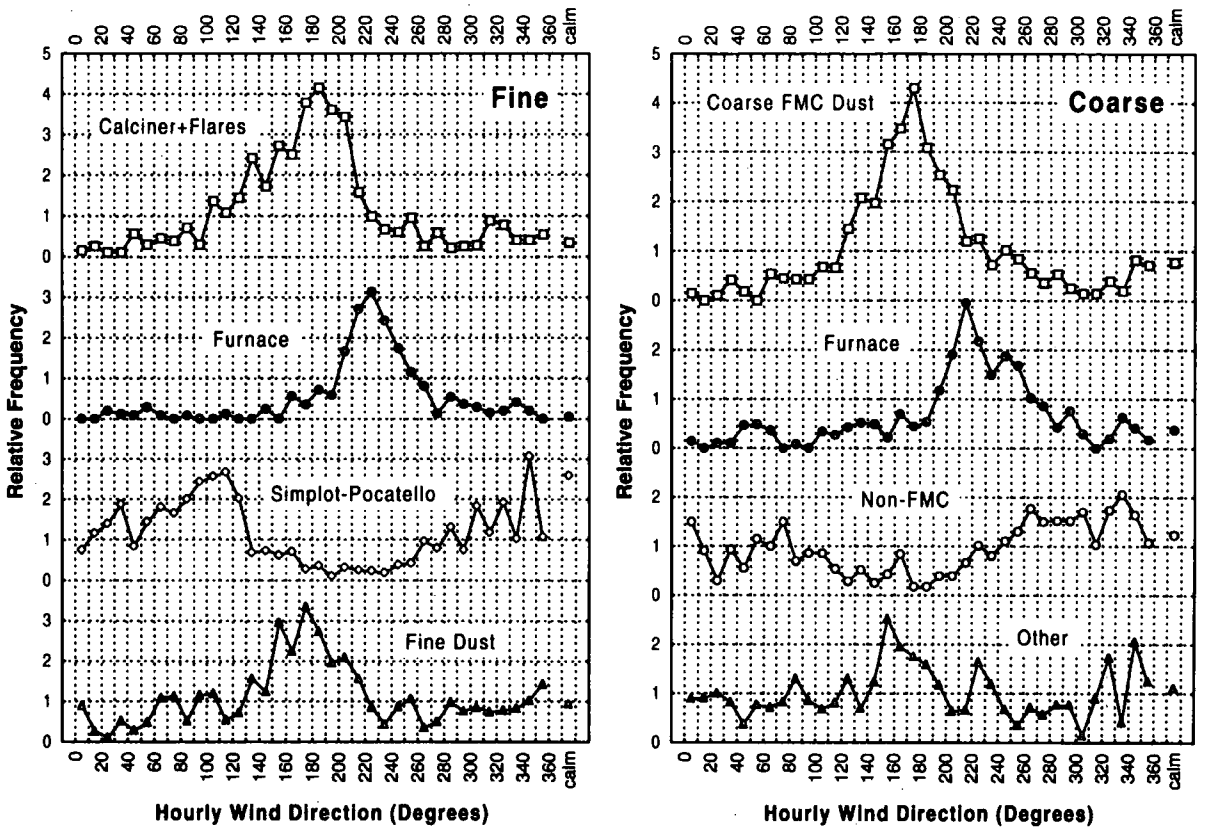

Figure 11. Relative frequency plots for fine-fraction (left) and coarse-fraction (right) UNMIX factors. For each factor, hourly wind direction data were compiled from the 20 dichot samples with the highest predicted mass contributions for that factor (90th percentile).